12-1-83 JS (i)

I-12339

Dr. 1957-7

ORNL/FEDC-83/3

SYSTEM STUDIES FOR A QUASI-STEADY-STATE ADVANCED PHYSICS TOKAMAK

R.L. REID
Y-K.M. PENG

MASTER

FUSION ENGINEERING DESIGN CENTER

Oak Ridge National Laboratory * Oak Ridge, Tennessee

ORNL/FEDC--83/3

DE84 002996

ORNL/FEDC-83/3
Dist. Category UC-20 c, d

SYSTEM STUDIES FOR A QUASI-STEADY-STATE ADVANCED PHYSICS TOKAMAK

Date Published - November 1983

R. L. Reid

Y-K. M. Peng

NOTICE This document contains information of a preliminary nature. It is subject to revision or correction and therefore does not represent a final report.

Prepared by the
OAK RIDGE NATIONAL LABORATORY
Oak Ridge, Tennessee 37830
operated by
UNION CARBIDE CORPORATION
for the
U.S. DEPARTMENT OF ENERGY
under Contract No. W-7405-eng-26

CONTENTS

ABSTRACT 1

I. INTRODUCTION 2

II. GUIDELINES AND CONSTRAINTS 3

III. IMPACT OF q_ψ, κ, Q, AND B_{max} 3

IIIA. Impact of Safety Factor q_ψ 4

IIIB. Impact of Plasma Elongation κ 5

IIIC. Impact of Power Amplification Q 6

IIID. Impact of Maximum TF Field B_{max} 7

IV. IMPACT OF REDUCING MAJOR RADIUS WITH PARTIAL NONINDUCTIVE STARTUP 9

V. IMPACT OF USING TUNGSTEN INBOARD SHIELDING 11

VI. REFERENCE PARAMETERS FOR AN ADVANCED PHYSICS TOKAMAK 11

VII. CONCLUSIONS 12

REFERENCES 14

APPENDIX 29

LIST OF FIGURES 34

ABSTRACT

Parametric studies were conducted using the Fusion Engineering Design Center (FEDC) Tokamak Systems Code to investigate the impact of variation in physics parameters and technology limits on the performance and cost of a low q_ψ, high beta, quasi-steady-state tokamak for the purpose of fusion engineering experimentation. The features and characteristics chosen from each study were embodied into a single Advanced Physics Tokamak design for which a self-consistent set of parameters was generated and a value of capital cost was estimated.

I. INTRODUCTION

Systems trade-off studies defining the impact of variation in physic parameters and technology limits were conducted for a low q_ψ (safety factor), quasi-steady-state tokamak through the use of the Fusion Engineering Design Center (FEDC) Systems Code (1). Low q_ψ is desirable in that reducing the value of q_ψ allows a higher beta limit; low q_ψ (less than 2) also achieves a reduction in plasma disruptivity [e.g., DIVA (2) and DIII (3)]. High beta serves to improve fusion performance and reduce device size while reduced disruptivity improves the reactor relevance of the tokamak concept.

Quasi-steady-state operation is predicated on utilizing rf current drive in conjunction with conventional inductive means to initiate and maintain plasma current. Recent successful demonstration on lower hybrid current drive in PLT (4), Alcator C, Versator II (5), and JIPP T-II (6), albeit at modest plasma densities, has introduced such a possibility. A proposed plasma operating scenario consists of alternating cycles of high density plasma burn (~1000 s) during which time plasma current is maintained by flux linkage from the ohmic heating solenoid followed by a period of low density rf current device plasma operation (~100 s) during which time the ohmic heating (OH) solenoid is recharged for the next high density plasma burn cycle.

The major topics addressed in these sensitivity studies are depicted in Fig. 1 and are summarized as follows:

- impact of the safety factor q_ψ, plasma elongation κ, and the maximum field at the toroidal field (TF) coil B_{max} on performance and cost;
- impact of the plasma power amplication factor Q on cost;
- impact of providing partial noninductive current startup on performance and cost; and
- impact of tungsten inboard shielding on performance and cost.

The features and characteristics chosen from each trade study were embodied into a single design. The parameters, performance, and cost of this Advanced Physics Tokamak configuration were determined and are included in the Appendix.

II. GUIDELINES AND CONSTRAINTS

The following general guidelines were adopted for the Advanced Physics Tokamak trade studies:

- startup and 100 s of burn provided by a conventional poloidal field (PF) system;
- 1000 s of burn provided by partial noninductive current drive;
- 30,000 cycles (at 1000 s of burn per cycle);
- slow (20-s) plasma current startup with rf assist or current drive (7);
- all external superconducting PF coils (relative to the TF coils);
- a maximum field of 8 T in the OH solenoid;
- pumped limiter impurity control system;
- plasma heating provided by rf injection;
- magnetic field ripple at the plasma edge maintained at a value of 1.0% (peak-to-average) or less;
- plasma average temperature set at 10 keV;
- energy confinement time based on INTOR scaling (8);
- $\varepsilon\beta_p = 0.50$, where ε is the inverse aspect ratio and β_p is the poloidal beta, so that $\beta \propto (1 + \kappa^2)$, where κ is elongation (9);
- separate vacuum boundary for torus and TF coils.

III. IMPACT OF q_ψ, κ, Q, AND B_{max}

Trade studies to determine the impact of q_ψ, κ, Q, and B_{max} on tokamak performance and cost were estimated using the FEDC Systems Code. The methodology used in these studies is to set a plasma minor radius leading to a neutron wall load. The thickness of the inboard bulk shielding is then made consistent with the radiation damage criterion of the TF coil insulation. The plasma aspect ratio is finally set to satisfy plasma current startup and 100-s inductively maintained burn time. Equilibrium field (EF) coil currents in the FEDC Systems Code are scaled as a function of plasma current and coil locations from reference values consistent with MHD equilibrium calculations. Reference EF configurations were defined by these MHD calculations for values of plasma elongation of 1.2, 1.4, and 1.6 for use in these studies.

IIIA. Impact of Safety Factor q_ψ

This study was done for a near-circular, natural plasma shape characterized by a plasma elongation of 1.2 and for a maximum field of 8 T at the TF coils. This natural shape can be provided by a relatively simple PF system consisting of two EF ring coils and an ohmic heating solenoid. The reference PF configuration used in this study is shown schematically in Fig. 2. Figure 3 shows the influence of q_ψ on neutron wall loading, relative cost, fusion power, and Q for a plasma minor radius of 1.2 m. Note that capital cost is normalized to the value achieved at $q_\psi = 2.1$. Decreasing the value of q_ψ for fixed plasma minor radius achieves substantial increases in Q, fusion power, and neutron wall loading, for relatively small increases in capital cost. Decreasing the value of plasma minor radius at a given value of q_ψ results in decreased Q, power, wall loading, and cost, as indicated by comparing results of Figs. 3, 4, and 5 for a plasma minor radius of 1.2, 1.0, and 0.8 m, respectively.

It is of interest then to compare costs at constant performance. Table I shows self-consistent parameters for a constant value of Q equal to 5 for values of plasma minor radii of 1.2, 1.0, and 0.8 m. Relative capital cost is seen to decrease with decreasing values of plasma minor radii achieved by decreasing values of q_ψ. Cost is decreased by 13% by a reduction in plasma minor radius from 1.2 to 0.8 m and a corresponding reduction in q_ψ from 2.06 to 1.46. Note that neutron wall loading increased from 0.42 to 0.62 MW/m^2 as the plasma minor radius and q_ψ decrease.

Table II is similar to Table I except that neutron wall loading is held constant at 0.5 MW/m^2 as the plasma minor radius is reduced from 1.2 to 0.8 m and the value of q_ψ is reduced from 1.96 to 1.55. The cost reduction with reduced q_ψ is also approximately 13%. Note that in this case, Q decreases as the plasma minor radius decreases.

The conclusion from this study is that for constant performance the lowest value of q_ψ allowed by plasma disruption and stabilizing criteria is desirable for capital cost minimization.

IIIB. Impact of Plasma Elongation κ

This study examines the influence of plasma elongation on performance and cost at a value of q_ψ of 2.1 for a maximum TF field of 8 T. The study was done for theoretical scaling of beta with plasma elongation at constant β_p which results in $\beta \propto (1 + \kappa^2)$ and for a more pessimistic scaling that beta is independent of plasma elongation. The latter scaling was modeled in the systems code by requiring $\beta_p \propto 1/(1 + \kappa^2)$. In conjunction with the independence of beta with elongation, energy confinement time was enhanced by a linear scaling with elongation, $\tau_E \propto \kappa$, as suggested by recent experiments (e.g., ISX-B).

The elongated plasma required additional shaping coils (relative to the near-circular configuration in Fig. 2) as shown in Figs. 6 and 7 for a reference PF configuration and for plasma elongations of 1.4 and 1.6, respectively. Note that these additional coils have currents in the same direction as the plasma current and hence reduce the next flux linkage to the plasma during startup. This must be compensated for by increasing the flux capability of the ohmic heating and outer EF coils by increasing the tokamak major radius, resulting in increased cost.

Figure 8 shows that relative cost, neutron wall loading, Q, and fusion power decrease with decreasing values of plasma minor radius for a fixed κ, assuming the more favorable scaling of β with κ. As κ is increased from 1.2 to 1.6, performance increases for a given value of the plasma minor radius but so does cost as is evident by comparing Figs. 8 through 10.

It is of interest to compare cost at constant performance. Table III shows self-consistent parameters for a value of Q ≈ 5 as κ is increased from 1.2 to 1.6. It is noted that as plasma elongation is increased, the minor radius decreases and the aspect ratio increases.

The effect of favorable scaling of beta with κ is essentially nullified by increased aspect ratio, which tends to lower beta. The net effect is that cost is essentially unchanged (~4%) as κ increases from 1.2 to 1.6. However, neutron wall loading does increase from 0.40 to 0.55 MW/m^2. This could be an important consideration for engineering testing applications. Table IV shows the breakdown of the direct captial cost for this variation of κ at constant Q.

Table V shows self-consistent parameters for a constant value of neutron wall loading of 0.5 MW/m^2 as κ is varied from 1.2 to 1.6. Again, cost is relatively insensitive to κ (~5%) over the variation considered. Note that increasing values of κ result in decreased values of Q at a constant value of neutron wall loading.

The effect of the alternate scaling of κ on β_p and τ_E [$\beta_p \propto 1/(1 + \kappa^2)$ with $\tau_E \propto \kappa$] for a constant value of Q = 5 is presented in Table VI. This scaling results in a cost increase of 18% as κ is increased from 1.2 to 1.6. Note that beta decreases due to an increased aspect ratio resulting from the κ increases.

The conclusions drawn from this study on the effects of plasma elongation are as follows:

1. Cost is insensitive to plasma elongation for a constant value of Q, assuming constant-β_p scaling of beta with κ. However, neutron wall loading scales favorably with elongation; and
2. assuming no beta improvement with elongation, near-circular plasmas are favored.

IIIC. Impact of Power Amplification Q

The change in relative capital cost as a function of Q for values of q_ψ of 1.8 and 2.1 is shown in Fig. 11. The maximum TF coil field is maintained at 8 T; Q is varied in the study by varying plasma minor radius. Aspect ratio is then determined consistent with maintaining flux linkage requirements from the PF system to provide 100 s of burn.

Figure 11 indicates that cost sensitivity to Q is a rather weak function. Q can be increased from a value of 5 to a value of 15 for an approximately 9% increase in capital cost. This result suggests that it should be cost-effective to require ignition as a nominal goal for the Advanced Physics Tokamak.

IIID. Impact of Maximum TF Field B_{max}

The impact of maximum TF field on performance and cost was investigated while maintaining $q_\psi = 1.8$ and $\kappa = 1.2$. Values of maximum TF fields of 8-12 T were chosen. The TF windings for the 8-10-T maximum field coils were composed of NbTi superconductor and copper. The 11- and 12-T winding featured a graded conductor with the 0-10 T portion being NbTi and copper and the high field portions being Nb_3Sn and copper.

The current densities and unit costs of the winding packs were varied as a function of maximum TF field. The cost of the winding packs was based on \$90/kg for NbTi and \$255/kg for Nb_3Sn conductor. The 11- and 12-T conductors were graded and costed assuming NbTi up to 10 T and Nb_3Sn for the remainder of the winding. The current density over the winding pack varies from 2500 A/cm^2 at 8 T to 2200 A/cm^2 at 10 T for the NbTi winding. For the graded conductor the current density for the NbTi portion is taken as 2200 A/cm^2, and the higher field Nb_3Sn portions vary from 1970 A/cm^2 at 11 T to 1700 A/cm^2 at 12 T. The resulting average windings pack current densities and unit costs are shown in Table VII as a function of maximum TF field.

The resulting relative capital cost as a function of maximum TF field and plasma minor radius is presented in Fig. 12. Note that 100 s of burn is maintained throughout by varying the plasma aspect ratio and that $\varepsilon\beta_p = 0.5$. In general, this figure shows that cost increases for an increasing minor radius (B_{max} constant) or for an increasing value of B_{max} (plasma minor radius constant). A boundary of marginal ignition is also shown on Fig. 12, relating maximum field, plasma size, and capital cost. Little capital cost difference is noted for configurations sized for 8 to 10 T, but going to 12 T requires a cost increase of $\sim$17% relative to the 10-T configuration. Tables VIII and IX present a summary of parameters and cost breakdown along the ignition boundary. It is seen that although the 10-T case suffers a

40% increase in TF coil cost from the 8-T case this increase is compensated for by a decreased cost of shield, PF coils, and electrical systems due to reduced minor radius (Table IX). This compensation is no longer effective for the 12-T case because of the overwhelming increase of TF coil cost (about 100%) over the 10-T case, coupled with a smaller reduction in other components. The latter results from an increase in major radius due to large increases in the TF coil build.

It is also of interest to determine the cost variation with maximum field at constant neutron wall loading. The boundaries for neutron wall loading of 1.0 and 1.5 MW/m^2 are shown in Fig. 13. It is seen that the capital cost achieves a minimum value at 10 T. At the 1.0-MW/m^2 level a cost increase of ∿10% is encountered by either decreasing B_{max} to 8 T or increasing B_{max} to 12 T.

For the constraints considered in this study, it appears that a value of B_{max} of 10 T is appropriate for the Advanced Physics Tokamak and that higher TF field strengths are not necessary or desired.

Because of the potential significance of this conclusion, it is of interest to assess its sensitivity to some of the assumptions imposed in this study. Figure 14 shows the impact of reducing the fixed value of $\epsilon\beta_p$ from 0.5 to 0.4 for tokamaks sized while achieving ignition and 100 s of burn. Again, the 10-T case achieves a minimum cost, which is about 20% below the 12-T case.

The sensitivity of this conclusion to the unit cost of Nb_3Sn was also assessed and is shown in Fig. 15. It is seen that if the unit cost of the Nb_3Sn and NbTi conductors are assumed to be the same, the relative total cost of the 12-T device would decrease from 1.26 to 1.17. This is still about 8% higher than the 10-T device, whose total relative cost is 1.08.

The effect of varying B_{max} on unit capital cost (capital cost divided by the plasma fusion power) is also examined. Figure 16 shows that the unit capital cost generally decreases as either plasma minor radius increases with constant B_{max} or as maximum field increases with constant plasma minor radius. Again, an inductive plasma burn time of 100 s and an $\epsilon\beta_p$ of 0.5 are maintained. The boundary of marginal ignition is also indicated in Fig. 16. It is seen that the unit capital cost increases 2% by going from 8 to 10 T. However, a unit capital cost increase of ~10% is incurred by going from 10 to 12 T. Therefore, the conclusion of B_{max} = 10 T being near optimal for FED-A is not sensitive to the assumed values of $\epsilon\beta_p$, the superconductor cost, or whether the optimization is based on capital cost or unit capital cost.

IV. IMPACT OF REDUCING MAJOR RADIUS WITH PARTIAL NONINDUCTIVE STARTUP

The purpose of these calculations is to determine the impact of relaxing the induction requirement for startup and 100 s of burn in the Advanced Physics Tokamak. Removing this requirement would allow the OH solenoid to be reduced with an accompanying reduction in the major radius. The reduced flux from the smaller sized solenoid is assumed to be augmented by noninductive current drive in order to achieve startup and maintain burn at desired values.

This study was done for three cases. In the first case, we maintained a constant plasma minor radius as the major radius was reduced, allowing the inductive startup and burn capability to decrease. This is expected to decrease plasma performance due to decreased toroidal field at the plasma with B_{max} kept constant. In the second case, we maintained a constant neutron wall loading by increasing the plasma minor radius as the major radius and the OH solenoid were reduced. In the third case, we maintained constant Q (i.e., ignition) by increasing the plasma minor radius as the major radius was decreased. Common constraints to each case include B_{max} = 8 T and q_ψ = 2.1.

Results for a constant plasma minor radius at 1.2 m are presented in Fig. 17. It shows that cost can be reduced approximately 25% by reducing the major radius from 4.3 to 2.8 m. However, at a major radius of 2.8 m performance is greatly decreased; fusion power is approximately 15 MW, compared with 112 MW at a 4.3-m major radius, and neutron wall loading is approximately 0.1 MW/m^2, compared with 0.4 MW/m^2 at 4.3 m major radius. The maximum field in the ohmic heating solenoid was maintained at 7 T as the major radius was reduced. At a major radius of 3.24 m, the bore of the solenoid consisted only of space for the solenoid winding plus gaps. Beyond this major radius, the solenoid field is reduced to zero and the reduction in major radius continued until the center of the device consisted only of a solid bucking cylinder. The conclusion drawn is that reduction of the major radius, even to the extreme where the OH solenoid is removed, is not cost-effective due to the deleterious impact on performance.

Results for constant neutron wall load are shown in Fig. 18. The major radius was reduced from 4.3 to 3.8 m at a constant neutron wall loading of 0.4 MW/m^2. Below a major radius of 3.8 m, a value of neutron wall loading of 0.4 MW/m^2 could not be achieved under the constraints of a fixed B_{max} and a fixed value of beta poloidal times inverse aspect ratio. Cost decreases with decreasing major radius and achieves a shallow minimum by only 4%. Further reduction in the major radius requires a cost increase in the EF coils, electrical systems, shield, and facilities that more than compensates for the cost reduction in the TF coils and heating system, as shown in Table X. Assuming the requirement of constant neutron wall loading, reducing the plasma major radius does not provide a significant cost saving even when the cost of noninductive current startup is ignored.

Results for constant Q are shown in Fig. 19. The major radius was reduced from 4.63 to 3.52 m while maintaining ignition conditions. Under these conditions, a 14% reduction in cost was achieved but at a reduced neutron wall loading (1.13 MW/m^2 as opposed to 0.89 MW/m^2). Further reduction in the major radius results in a cost increase. Again, the flux linkage from the PF system was not required to provide full inductive startup and burn as the major radius was decreased. A cost breakdown by system and selected plasma parameters is shown in Tables XI and XII as a function of major radius. The low aspect ratio encountered at reduced major radii provides poor utilization of the maximum TF field but does allow high values of beta as seen in Table XII. Assuming the requirements of constant performance, characterized by ignition, reducing the plasma major radius and assuming partial noninductive startup provides a significant cost saving.

V. IMPACT OF USING TUNGSTEN INBOARD SHIELDING

The use of tungsten as the inboard shield material allows the thickness of the shield to be reduced due to the enhanced neutron attenuation of tungsten relative to stainless steel. For this study, the e-fold thickness (the thickness required to attenuate the neutron flux by a factor of 2.718) of tungsten was taken to be 75% of the e-fold distance of stainless steel.

Tokamak configurations, at ignition and for a maximum TF field of 10 T, that utilize stainless steel and tungsten inboard shields are presented in Table XII. The tungsten shield is thinner by 14 cm than a stainless steel shield, leading to a reduction in the tokamak major radius of 25 cm. However, the unit cost of fabricated tungsten is about twice that of stainless steel, and the density of tungsten is about twice that of stainless steel. For the same volume, the cost of tungsten would therefore be approximately four times that of steel. The net impact of this shield material is found to be 2% in favor of the tungsten shield, as shown in Table XIII. The reduced cost of the smaller tokamak components utilizing the tungsten inboard shield is essentially nullified by the higher cost of the tungsten shield itself, as shown in Table XIV.

It is concluded that the choice of shield material has little impact on total capital cost, at least for the size device considered in this study.

VI. REFERENCE PARAMETERS FOR AN ADVANCED PHYSICS TOKAMAK

A set of reference parameters for an Advanced Physics Tokamak is chosen based on the results of the trade studies and is presented in the Appendix. The parameters include a maximum field of 10 T, a plasma safety factor of 1.8, and 12 TF coils with size limited by the ripple requirement; ignition is assumed. In addition, two desirable features were included in the reference parameters that were not assumed in the trade studies: (1) a forced flow OH solenoid and (2) a combined vacuum boundary. A forced flow OH solenoid allows the space between the bucking cylinder and winding pack to be reduced by 10 cm, relative to that required by a pool-boil design, providing a greater flux capability. A combined vacuum boundary, as opposed to the separate vacuum boundaries for the torus and TF coils, allows a savings of 15 cm in the inboard radial build of the tokamak. The direct capital cost of this version of an Advanced Physics Tokamak is estimated to be $729 million or about 70% of the cost of the 1981 FED baseline design (10), which is a moderate q_ψ device (q = 3.2) with comparable performance goals. A cost breakdown by component is included in the Appendix.

VII. CONCLUSIONS

The conclusions drawn from the trade studies for a quasi-steady-state Advanced Physics Tokamak are summarized as follows.

1. The capital cost decreases with decreasing q_ψ for constant Q or constant neutron wall loading. A 13% cost reduction is indicated when q_ψ is reduced from 2.0 to 1.5.
2. Cost is insensitive to plasma elongation at a constant value of Q, assuming the theoretical scaling of beta; however, the neutron wall loading scales nearly linearly with elongation κ.
3. Assuming no beta improvement with elongation, near-circular plasmas are favored.
4. A maximum TF field of 10 T appears to be optimum for an Advanced Physics Device on the basis of capital cost and unit capital cost for marginal ignition or for constant neutron wall loading, subject to the constraint of inductive startup and 100 s of burn. For marginal ignition, a cost increase of 17% is observed in going from 10 to 12 T. At a constant neutron wall loading of 1.0 MW/m^2, the cost increase is 10%.
5. The cost impact of tungsten inboard shielding, compared with stainless steel, is slight (approximately 2% when marginal ignition requirements and 10-T maximum TF fields are maintained).
6. Providing partial noninductive current startup is moderately cost-effective (∿15%) by allowing a reduced major radius and a reduced flux OH solenoid while maintaining marginal ignition and a maximum TF field of 10 T. For a constant neutron wall loading, partial

noninductive startup is not cost-effective and full OH solenoid capability should be maintained.

7. High Q (∿15), brought about by increasing the plasma size, requires only a modest increase in capital cost (∿10%) relative to the case of Q = 5.

8. A combination of features such as low q, slow plasma startup, natural plasma shape, and combined vacuum boundary allows a capital cost reduction of ∿30% for an Advanced Physics Tokamak relative to the 1981 FED baseline configuration, a moderate q_ψ device with comparable performance goals.

1. R. L. REID and D. STEINER, Parametric Studies for the Fusion Engineering Device, Nucl. Tech./Fusion 4 (July 1983).

2. DIVA GROUP, Nucl. Fusion 20, 271 (1980).

3. T. OKWAWA and D-III GROUP, 9th International Conference on Plasma Physics and Controlled Nuclear Fusion, Baltimore, Maryland, 1982, Paper IAEA-CN-41/A-2.

4. W. HOOKE, 9th International Conference on Plasma Physics and Controlled Nuclear Fusion, Baltimore, Maryland, 1982, Paper IAEA-CN-41/c-5.

5. M. PORKOLAB, 9th International Conference on Plasma Physics and Controlled Nuclear Fusion, Baltimore, Maryland, 1982, Paper IAEA-CN-41/c-4.

6. T. AMANO, 9th International Conference on Plasma Physics and Controlled Nuclear Fusion, Baltimore, Maryland, 1982, Paper IAEA-CN-41/c-3.

7. S. K. BOROWSKI, Y-K. M. PENG, and T. KAMMASH, "RF-Assisted Current Startup in the Fusion Engineering Device (FED)," ORNL/TM-8319, Oak Ridge National Laboratory (August 1982).

8. W. M. STACEY et al., "The US Contribution to the International Tokamak Reactor Phase-1 Workshop," INTOR/81-1, (June 1981).

9. C. A. FLANAGAN, D. STEINER, and G. E. SMITH, "Initial Trade Studies for the Fusion Engineering Device," ORNL/TM-7777, Oak Ridge National Laboratory (June 1981).

10. C. A. FLANAGAN, D. STEINER, and G. E. SMITH, "Fusion Engineering Device Design Description," Vols. 1 and 2, ORNL/TM-7948, Oak Ridge National Laboratory (December 1981).

Table I. Parameters and cost for near-circular plasma at a value of Q = 5.0

	Plasma minor radius, a (m)		
	1.2	1.0	0.8
κ	1.2	1.2	1.2
A	3.62	4.10	4.82
R_o (m)	4.34	4.10	3.86
q_ψ	2.06	1.76	1.46
β (%)	6.6	7.4	8.5
B_T (T)	3.43	3.55	3.68
B_{max} (T)	8.0	8.0	8.0
I_p (MA)	4.4	3.7	3.0
P_{th} (MW)	120	115	105
L_w (MW/m^2)	0.42	0.50	0.62
$\$_R$	1.005	0.940	0.875

Table II. Parameters and cost for a near-circular plasma at a constant value of L_w = 0.5 MW/m^2

	Plasma minor radius, a (m)		
	1.2	1.0	0.8
κ	1.2	1.2	1.2
A	3.67	4.10	4.75
R_o (m)	4.40	4.10	3.80
q	1.96	1.76	1.55
β (%)	7.1	7.4	7.7
B_T (T)	3.46	3.55	3.64
B_{max} (T)	8.0	8.0	8.0
I_p (MA)	4.5	3.7	2.9
P_{th} (MW)	150	115	80
Q	7.5	5	3
$\$_R$	1.015	0.940	0.872

Table III. Comparison of elongated and near-circular plasmas for Q = 5 (theoretical beta scaling) with B_{max} = 8.0 T $\epsilon\beta_p$ = 0.5, and T_B = 100 s

	Plasma elongation, κ		
	1.2	1.4	1.6
q	1.2	1.2	1.2
a (m)	1.2	1.06	0.93
A	3.6	4.2	4.7
R_o (m)	4.32	4.45	4.37
β (%)	6.4	6.1	6.2
B_T (T)	3.42	3.78	3.92
I_p (MA)	4.3	4.2	3.9
P_{th} (MW)	115	135	150
L_w (MW/m^2)	0.40	0.50	0.55
$\$_R$	1.0	1.03	1.04

Table IV. Summary of cost (in millions of dollars) for elongated and near-circular plasmas for $Q = 5$ with $B_{max} = 8.0$ T, $q = 2.1$, $\epsilon\beta_p = 0.5$, and $T_B = 100$ s

	Plasma elongation, κ		
	1.2	1.4	1.6
Shield	50.0	51.9	52.0
TF coils	66.7	73.0	72.7
PF coils	46.7	48.2	48.2
Plasma heating	66.4	72.7	78.5
Electrical	23.0	23.6	23.7
Heat transport	14.8	16.8	18.0
Facilities	143.8	143.6	142.4
Other	154.9	155.9	156.0
Total	566.3	585.7	591.5
Relative cost	1.0	1.03	1.04

Table V. Comparison of elongated and near-circular plasmas for L_w = 0.5 MW/m^2 with B_{max} = 8.0 T, $\varepsilon\beta_p$ = 0.5, and T_B = 100 s

	Plasma elongation, κ		
	1.2	1.4	1.6
q	2.1	2.1	2.1
a (m)	1.32	1.06	0.90
A	3.45	4.2	4.78
R_o (m)	4.55	4.45	4.30
β (%)	6.9	6.1	6.1
B_T (T)	3.41	3.78	3.92
I_p (MA)	5.0	4.2	317
P_{th} (MW)	160	135	130
Q	9	5	4
$\$_R$	1.06	1.04	1.01

Table VI. Comparison of elongated and near-circular plasmas for Q = 5 assuming beta is independent of κ with B_{max} = 8.0 T and T_B = 100 s

	Plasma elongation, κ		
	1.2	1.4	1.6
q	2.1	2.1	2.1
$\epsilon\beta_p$	0.50	0.37	0.29
a (m)	1.2	1.19	1.17
A	3.6	3.99	4.24
R_o (m)	4.32	4.75	4.96
β (%)	6.4	4.9	4.2
B_T (T)	3.42	3.83	4.03
I_p (MA)	4.3	5.0	5.8
P_{th} (MW)	115	130	135
L_w (MW/m^2)	0.40	0.38	0.35
$\$_R$	1.00	1.11	1.18

Table VII. Current density and unit cost as a function of maximum toroidal field assumed in the system analysis

B_{max} (T)	J_{Nb_3Sn} (A/cm^2)	J_{wp}[a] (A/cm^2)	$/$kg_{wp}$	Conductor composition
12	1700	2100	124	Nb_3Sn, NbTi, Cu
11	1970	2177	107	Nb_3Sn, NbTi, Cu
10		2200	90	NbTi, Cu
9		2370	90	NbTi, Cu
8		2500	90	NbTi, Cu

[a] Winding pack overall current density.

Table VIII. Ignition FED-A parameters vs B_{max}, where $q_{\psi} = 1.8$, $\kappa = 1.2$, $\epsilon\beta_p = 0.5$, and $T_B = 100$ s

	B_{max} (T)		
	8	10	12[a]
J_{wp} (A/cm^2)	2500	2200	2100
J_{OA} (A/cm^2)	1675	1515	1245
TF coil megampere-turns	82	115	163
a (m)	1.29	0.97	0.77
A	3.62	4.77	6.35
R_o (m)	4.67	4.63	4.89
β (%)	8.6	5.7	4.0
B_T (T)	3.51	4.96	6.69
I_p (MA)	5.5	4.1	3.2
PF flux (Wb)	84	73	70
L_p (MW/m^2)	0.86	1.13	1.42
P_{fus} (MW)	280	275	290
S_R	1.09	1.08	1.26

[a] Graded NbTi/Nb_3Sn.

Table IX. Cost summary at marginal ignition as a function of B_{max}

	B_{max} (T)		
	8	10	12
Shield	60.4	51.8	49.3
TF coils	81.0	113.1	223.0
PF coils	61.3	44.0	35.7
Plasma heating	60.0	59.2	61.3
Electrical	39.9	31.9	29.4
Heat transport	20.7	21.0	23.4
Facilities	148.3	143.6	143.2
Other	146.4	146.3	147.6
Total	618.0	610.9	712.9
Relative cost	1.09	1.08	1.26

Table X. Summary of costs (in millions of dollars) for variation in major radius at constant neutron wall loading (partial noninductive current start-up)

	R_o = 4.32 m	R_o = 4.0 m	R_o = 3.8 m
Shield	50.0	49.3	53.7
TF system	66.7	51.3	36.5
PF system	46.6	48.4	62.5
Heating system	66.4	61.1	56.9
TF electrical system	19.2	20.8	32.0
Facility	143.8	143.3	146.9
Other	173.6	171.3	170.3
Total cost	566.3	545.5	558.8
Relative cost	1.0	0.963	0.987

Table XI. Summary of costs (in millions of dollars) for variation in major radius at ignition (partial noninductive current startup)

	R_o = 4.63 m	R_o = 3.65 m	R_o = 3.52 m
Shield	51.8	44.7	45.2
TF system	113.1	54.9	46.6
PF system	44.0	41.2	44.7
Heating system	59.2	52.0	51.2
PF electrical system	18.7	18.8	22.5
Facility	143.6	139.4	140.2
Other	180.6	170.6	169.8
Total cost	611.0	521.6	520.2
Relative cost	1.08	0.922	0.919

Table XII. Selected parameters as a function of major radius for ignited plasmas (partial noninductive current startup)

	Major radius, R (m)		
	4.63	3.65	3.52
A	4.77	3.17	2.82
a (m)	0.97	1.15	1.25
q_ψ	1.8	1.8	1.8
Beta (%)	5.7	10.9	13.8
B_T (T)	4.96	3.29	2.82
B_{max} (T)	10	10	10
I_p (MA)	4.1	5.5	6.1
P_{th} (MW)	275	215	210
L_w (MW/m^2)	1.13	0.95	0.89

Table XIII. Comparison of inboard shield configurations at ignition (B_{max} = 10 T, q = 1.8, T_B = 100 s)

Parameter	Reference stainless steel shield	Tungsten shield
Δ_s (m)	0.58	0.44
a (m)	0.95	0.895
A	4.82	4.84
R_o (m)	4.58	4.33
β (%)	5.6	5.6
B_T (T)	4.97	5.13
I_p (MA)	3.98	3.86
P_{fus} (MW)	255.0	241.0
L_p (MW/m^2)	1.08	1.15
$\$_R$	1.064	1.047

Table XIV. Summary of cost (in millions of dollars) for stainless steel vs tungsten shield

	Reference stainless steel	Tungsten 90%
Shield	50.5	63.8
TF coils	110.2	99.1
PF coils	42.3	38.4
Plasma heating system	59.1	57.2
Electrical system	31.2	29.5
Heat transport	20.3	19.4
Facilities	143.0	140.3
Other	145.9	145.0
Total	602.5	592.7
$\$_R$	1.064	1.047

APPENDIX

Table A.I. Reference parameters for an advanced physics tokamak

Description	Value
Geometry	
Major radius, R	4.22 m
Plasma radius, a	0.92 m
Plasma elongation, κ	1.2 m
Aspect ratio, A	4.59 m
Scrape-off layer	0.15 m
Plasma	
Average ion temperature, $\langle T_i \rangle$	10 keV
Safety factor (edge), q_ψ (flux-surface-averaged)	1.8
Effective charge (during burn), Z_{eff}	1.5
TF ripple (peak-to-average), edge	1.0%
Plasma current, I_p	4.1 MA
Average electron density, $\langle n_e \rangle$	1.7×10^{14} cm^{-3}
$\epsilon\beta_p$	0.5
Total beta, $\langle \beta \rangle$	6.0%
Toroidal field at plasma, B_T	4.98 T
Q	Ignited
Operating mode	
Burn time, t_{burn}	100 s, 1000 s[a]
Fusion power, P_{fus}	255 MW
Pumpdown time, t_p	30 s
Startup/shutdown time, t_{ss}	26 s/26 s
Number of full field current pulses/lifetime	3×10^4
Average number of burn pulses in each current pulse	10
Lifetime	10 years
Torus eddy current times (L/R)	
Conducting vessel	~1 s
Other conducting path	~0.2 s

Table A.I. (cont'd)

Description	Value
First wall/armor	
Coolant	H_2O
Average neutron wall load at plasma edge	1.2 MW/m^2
Average neutron wall load at first wall	1.0 MW/m^2
Average thermal wall load	TBD[b]
Shield	
Inboard shield material	Stainless steel
Inboard thickness (excluding spool armor, gaps, scrapeoff)	62 cm
Dose rate to TF coil insulation	1×10^9 rad
Time after shutdown to permit personnel access (2.5 mrem/h)	36 h
Outboard shield thickness (stainless steel)	120 cm
Maximum structure temperature	200°C
Vacuum	
Initial base pressure	10^{-7} torr
Preshot base pressure	10^{-5} torr
Postshot base pressure	3×10^{-4} torr
Pressure at duct inlet during burn	10^{-2} torr
Particle flux (molecular) to be pumped	$<10^{23}$ s^{-1}
TF coils	
Number	12
Peak design field at winding, B_m	10 T
Conductor winding current density, J_w	2200 A/cm^2
Overall current density, J_{OA}	1720 A/cm^2
PF coils	
Total flux capability	67 Wb
EF flux	24 Wb
OH flux	43 Wb
Total maximum ampere-turns	51 MAT
Maximum EF ampere-turns	6 MAT
Maximum OH ampere-turns	45 MAT

Table A.I. (cont'd)

Description	Value
OH maximum field allowable at coil	7 T
OH current ramp time	30 s
Conductor winding pack current density, J_{wp}	1400 A/cm^2
Plasma heating	
Startup	
Initiating voltage with rf assist only	<10 V
Current rise time	20 s
Startup ECH power	3.5 MW
Time duration for ECH assist	20 s
Frequency	120 GHz
Bulk heating (including startup)	Lower hybrid
Power	25 MW
Current drive	
Startup	
Lower hybrid current	
Rise time	20 s
Power	10-20 MW
Frequency	1-3 GHz
Others (REB, FWIC, ECH)	TBD[b]
Current maintenance	
Lower hybrid	
Power	25 MW
Frequency	1-5 GHz
Others (REB, FWIC, ECH)	TBD[b]

[a] 100 s provided by PF system in the absence of noninductive current drive, 1000 s with partial noninductive current drive.

[b] To be determined.

Table A.II. Cost estimate summary for an advanced physics tokamak

			FED-A	FED Baseline
1.	Magnet system		151.5	312.2
	TF coil	97.2		
	PF coil	35.1		
	Intercoil structure	4.0		
	Bucking cylinder	3.7		
	Cryostat	11.5		
2.	Torus		120.4	161.9
	Shell	17.7		
	Armor	0.7		
	Shield	86.8		
	Pumped limiter module	8.1		
	Torus support	7.1		
3.	Cooling systems		18.8	38.5
	Refrigeration	7.5		
	Heat transport loops	5.8		
	Cooling tower	5.5		
4.	Tritium and fuel handling		48.2	54.0
	Primary fuel cycle	6.4		
	Secondary systems	16.0		
	Tritium system data acquisition	9.1		
	Tritium cleanup (room)	12.7		
	Fuel injector	4.0		
5.	Plasma heating		97.3	89.0
	Bulk heating			
	LHRH	83.3		
	Shielding	2.1		
	Preheating (ECRH)	11.9		
6.	Electrical systems		29.0	99.1
	PF electrical	15.1		
	TF electrical	4.7		
	ac power	9.2		
7.	Vacuum pumping system		8.3	24.0
	Vacuum duct	4.1		
	Vacuum pumps	4.2		
8.	Instrumentation and control		67.0	67.0
	Diagnostics	42.0		
	Information and control systems	25.0		

Table A.II. (cont'd)

			FED-A	FED Baseline
9.	Maintenance equipment		60.4	60.4
	Reactor cell	33.3		
	Hot cell	27.1		
10.	Facilities		128.2	138.6
	Reactor cell	31.6		
	Hot cell	35.0		
	Cooling system structures	1.1		
	Cryogenic refrigeration building	1.0		
	Radiation waste building	4.3		
	Administration building	4.3		
	Mockup and shop building	13.5		
	Power supply and energy storage building	2.9		
	Diesel generator building	0.4		
	Tritium processing building	8.1		
	Ventilation building and stack	13.7		
	Site improvements	12.3		
Total direct cost			729.1	1044.7
11.	Indirect costs			
	Engineering and management (45%)		328.1	
	Installation (15%)		109.4	
	Total (direct + indirect)		1166.6	
	Contingency (30%)		350.0	
Total cost			1516.6	

FIGURE CAPTIONS

Fig. 1. Flow chart for FED-A trade studies.

Fig. 2. Reference PF system for a near-circular plasma.

Fig. 3. Performance and cost as a function of q_ψ for a plasma minor radius of 1.2 m.

Fig. 4. Performance and cost as a function of q_ψ for a plasma minor radius of 1.0 m.

Fig. 5. Performance and cost as a function of q_ψ for a plasma minor radius of 0.8 m.

Fig. 6. Reference PF system for a plasma elongation of 1.4.

Fig. 7. Reference PF system for a plasma elongation of 1.6.

Fig. 8. Performance and cost as a function of plasma minor radius at a constant value of κ of 1.2.

Fig. 9. Performance and cost as a function of plasma minor radius at a constant value of κ of 1.4.

Fig. 10. Performance and cost as a function of plasma minor radius at a constant value of κ of 1.6.

Fig. 11. Relative capital cost as a function of Q at constant value of B_{max} of 8 T.

Fig. 12. Relative capital cost as a function of plasma minor radius and maximum TF field. A boundary of marginal ignition is indicated.

Fig. 13. Relative capital cost as a function of plasma minor radius and maximum TF field. Lines of constant neutron wall loading are indicated.

Fig. 14. Relative capital cost as a function of $\epsilon\beta_p$ and maximum TF field.

Fig. 15. Relative capital cost as a function of the ratio of the unit conductor cost of Nb_3Sn to NbTi.

Fig. 16. Unit cost ($\$/kW_t$) as a function of plasma minor radius and maximum TF field. A boundary of marginal ignition is indicated.

Fig. 17. Relative capital cost, fusion power, neutron wall loading, and aspect ratio as a function of major radius for constant values of plasma minor radius and maximum TF field. The requirement for an inductive plasma current startup is relaxed as the major radius is reduced from 4.3 m.

Fig. 18. Relative capital cost, Q, minor radius, and aspect ratio as a function of major radius for a constant value of neutron wall loading. The requirement for an inductive plasma current startup is relaxed as the major radius is reduced from 4.3 m.

Fig. 19. Relative capital cost, neutron wall loading, minor radius, and aspect ratio as a function of major radius at ignition. The requirement for an inductive plasma current startup is relaxed as the major radius is reduced from 4.3 m.

FLOW CHART FOR FED-A TRADE STUDIES

ORNL-DWG 82-4125 FED

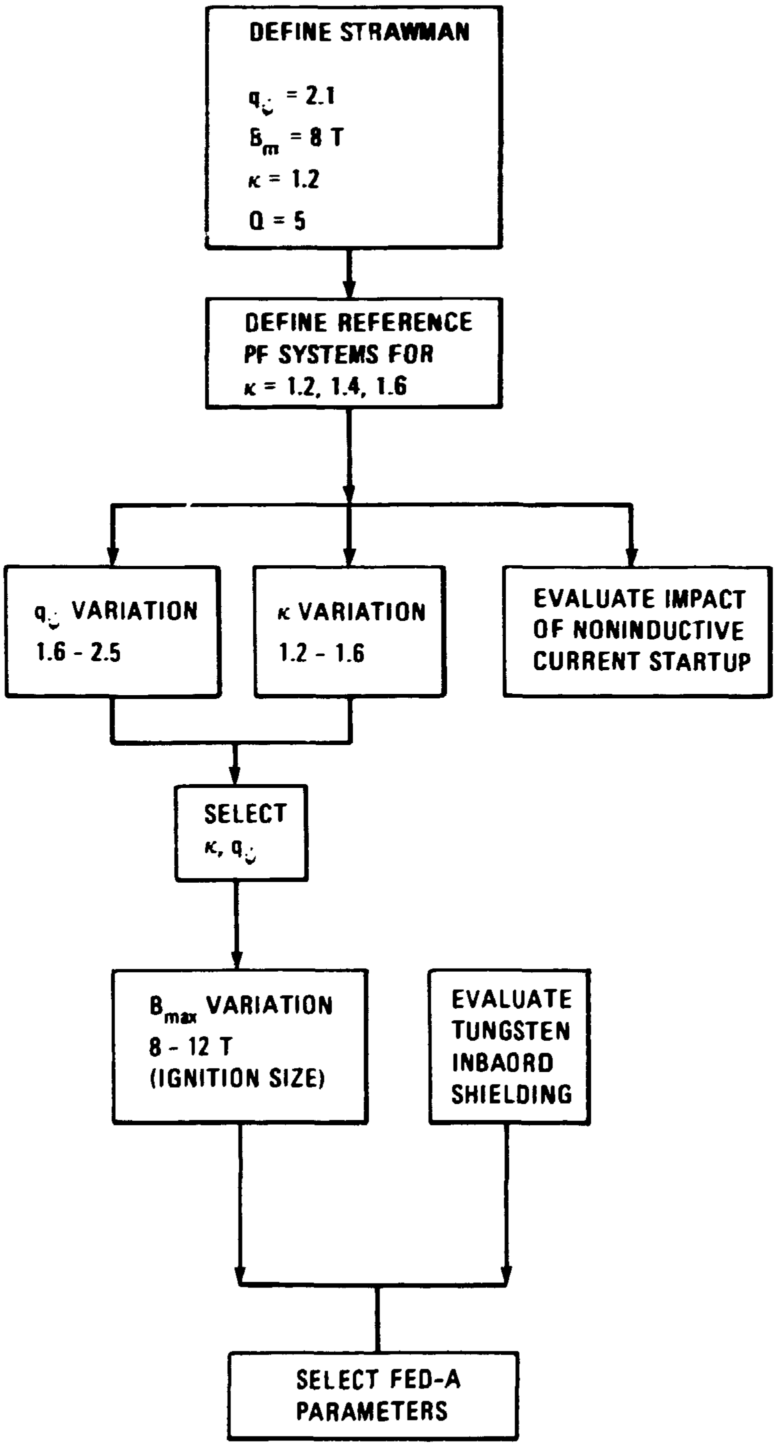

Fig. 1

REFERENCE PF SYSTEM FOR NEAR CIRCULAR PLASMA

ORNL-DWG 82-2580 FED

K = 1.2

a = 1.0 m

A = 4.0

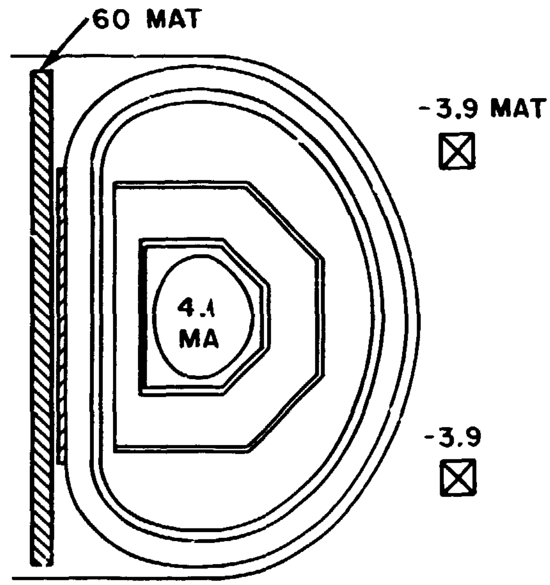

Fig. 2

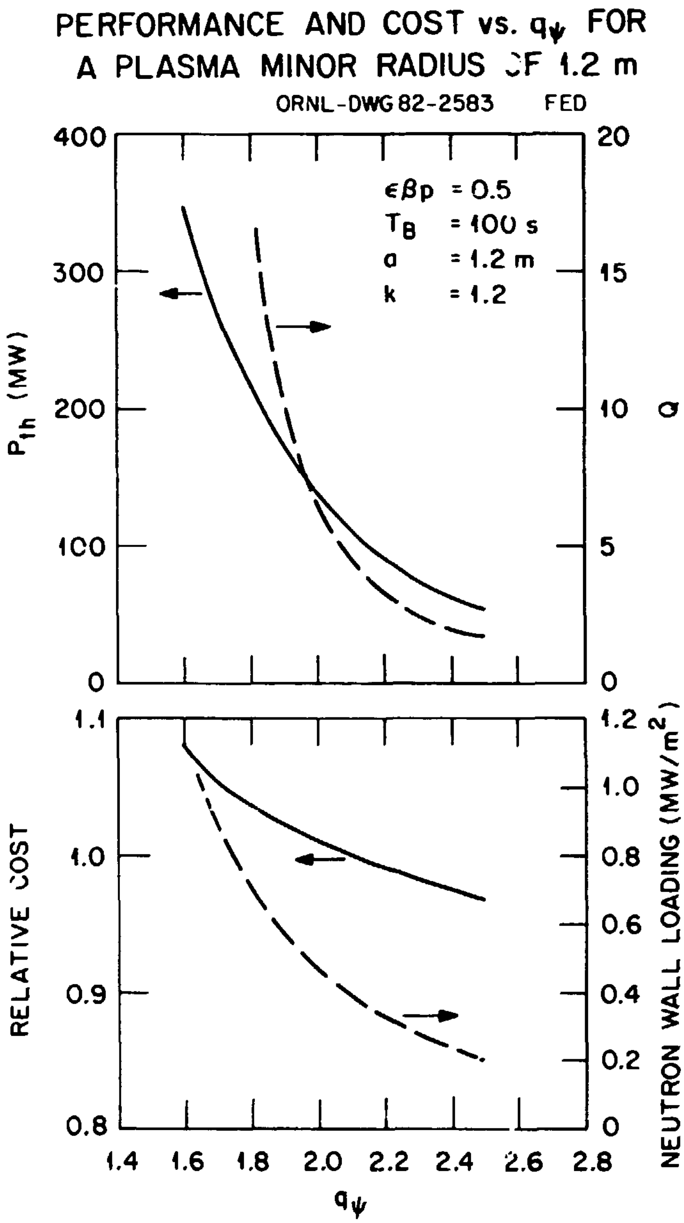
PERFORMANCE AND COST vs. qψ FOR
A PLASMA MINOR RADIUS OF 1.2 m
ORNL-DWG 82-2583 FED
εβp = 0.5
TB = 100 s
a = 1.2 m
k = 1.2
Pfh (MW)
Q
RELATIVE COST
NEUTRON WALL LOADING (MW/m2)
qψ
400
300
200
100
0
20
15
10
5
1.1
1.0
0.9
0.8
1.2
0.6
0.4
0.2
1.4
1.6
1.8
2.0
2.2
2.4
2.6
2.8

Fig. 3

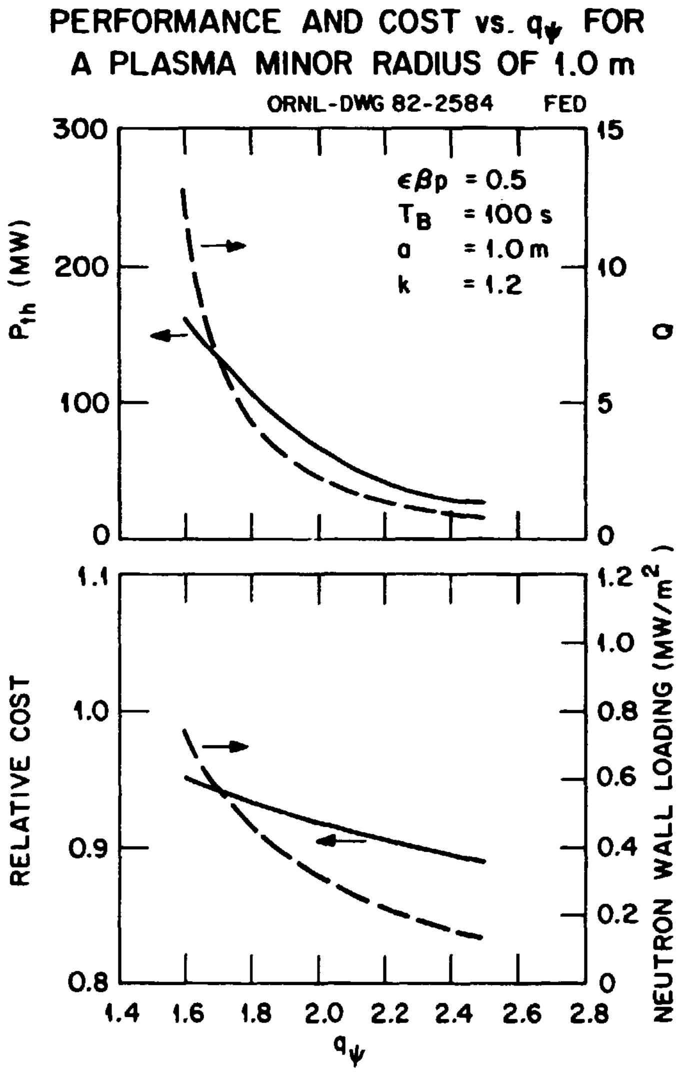
PERFORMANCE AND COST vs. q_ψ FOR
A PLASMA MINOR RADIUS OF 1.0 m
ORNL-DWG 82-2584 FED
$\epsilon\beta p$ = 0.5
T_B = 100 s
a = 1.0 m
k = 1.2
P_{th} (MW)
q
RELATIVE COST
NEUTRON WALL LOADING (MW/m^2)
q_ψ
300
200
100
0
15
10
5
0
1.1
1.0
0.9
0.8
1.2
1.0
0.8
0.6
0.4
0.2
0
1.4
1.6
1.8
2.0
2.2
2.4
2.6
2.8

Fig. 4

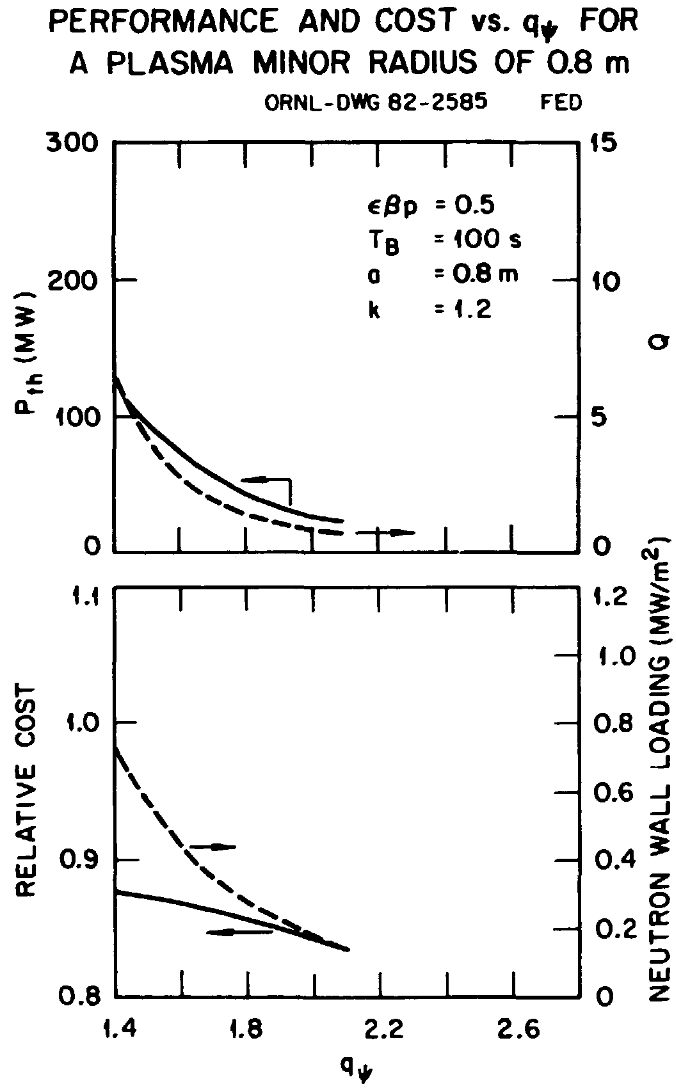
PERFORMANCE AND COST vs. q_ψ FOR
A PLASMA MINOR RADIUS OF 0.8 m
ORNL-DWG 82-2585 FED
$\epsilon\beta p$ = 0.5
T_B = 100 s
a = 0.8 m
k = 1.2
P_{th} (MW)
Q
RELATIVE COST
NEUTRON WALL LOADING (MW/m^2)
q_ψ
300
200
100
0
15
10
5
0
1.1
1.0
0.9
0.8
1.2
1.0
0.8
0.6
0.4
0.2
0
1.4
1.8
2.2
2.6

Fig. 5

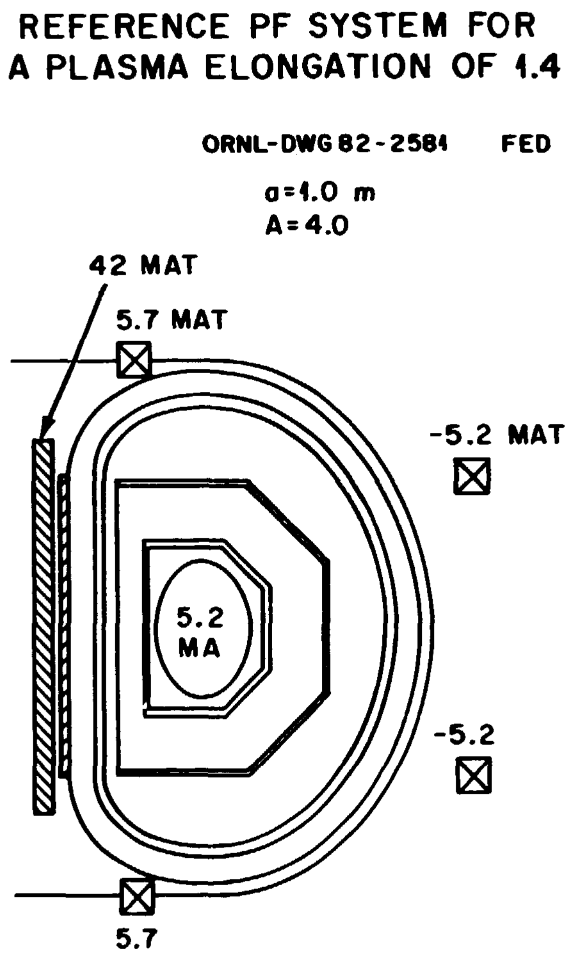
REFERENCE PF SYSTEM FOR
A PLASMA ELONGATION OF 1.4
ORNL-DWG 82-2584 FED
a=1.0 m
A=4.0
42 MAT
5.7 MAT
-5.2 MAT
5.2
MA
-5.2
5.7

Fig. 6

REFERENCE PF SYSTEM FOR
A PLASMA ELONGATION OF 1.6

ORNL-DWG 82-2582 FED

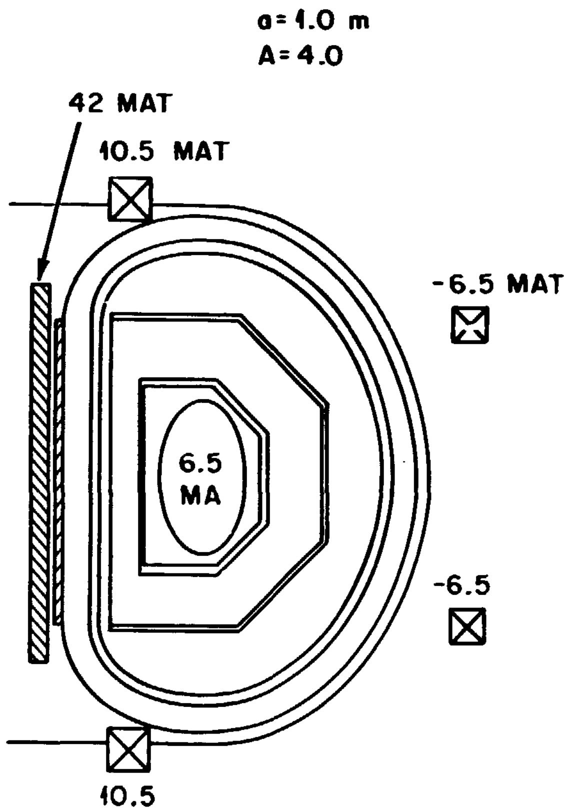

Fig. 7

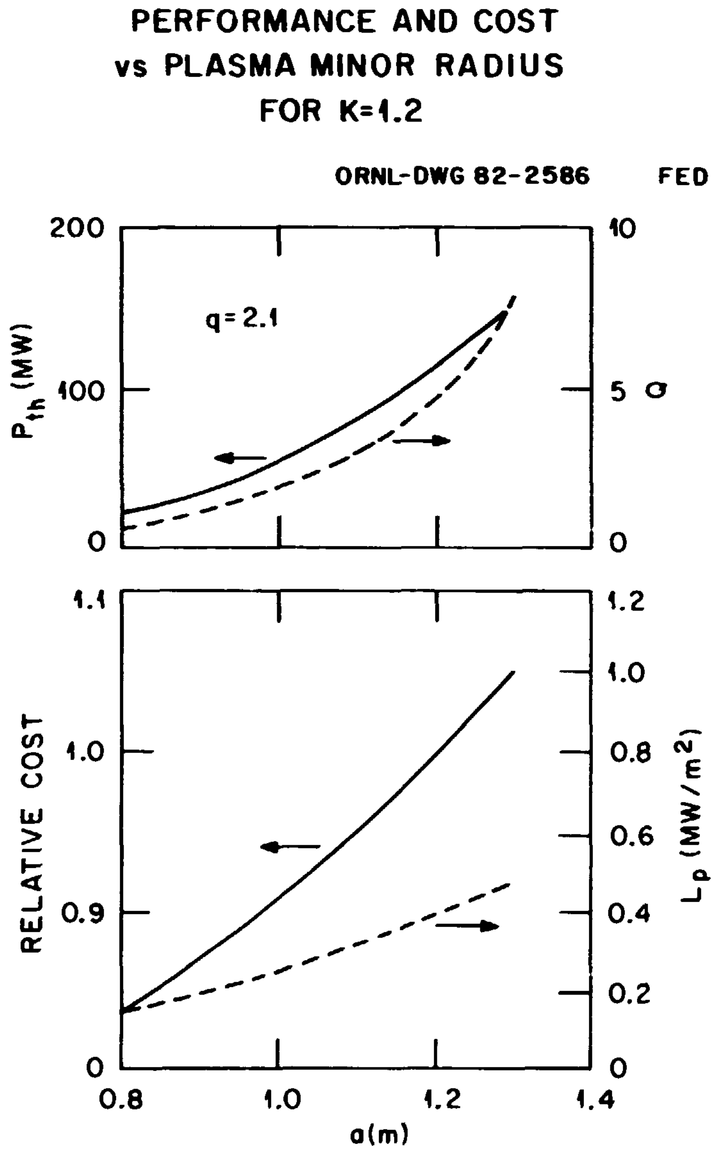

PERFORMANCE AND COST
vs PLASMA MINOR RADIUS
FOR K=1.2
ORNL-DWG 82-2586 FED
200
100
0
10
5
0
q=2.1
P_{th} (MW)
Q
1.1
1.0
0.9
0
1.2
1.0
0.8
0.6
0.4
0.2
0
RELATIVE COST
L_p (MW/m^2)
0.8
1.0
1.2
1.4
a(m)

Fig. 8

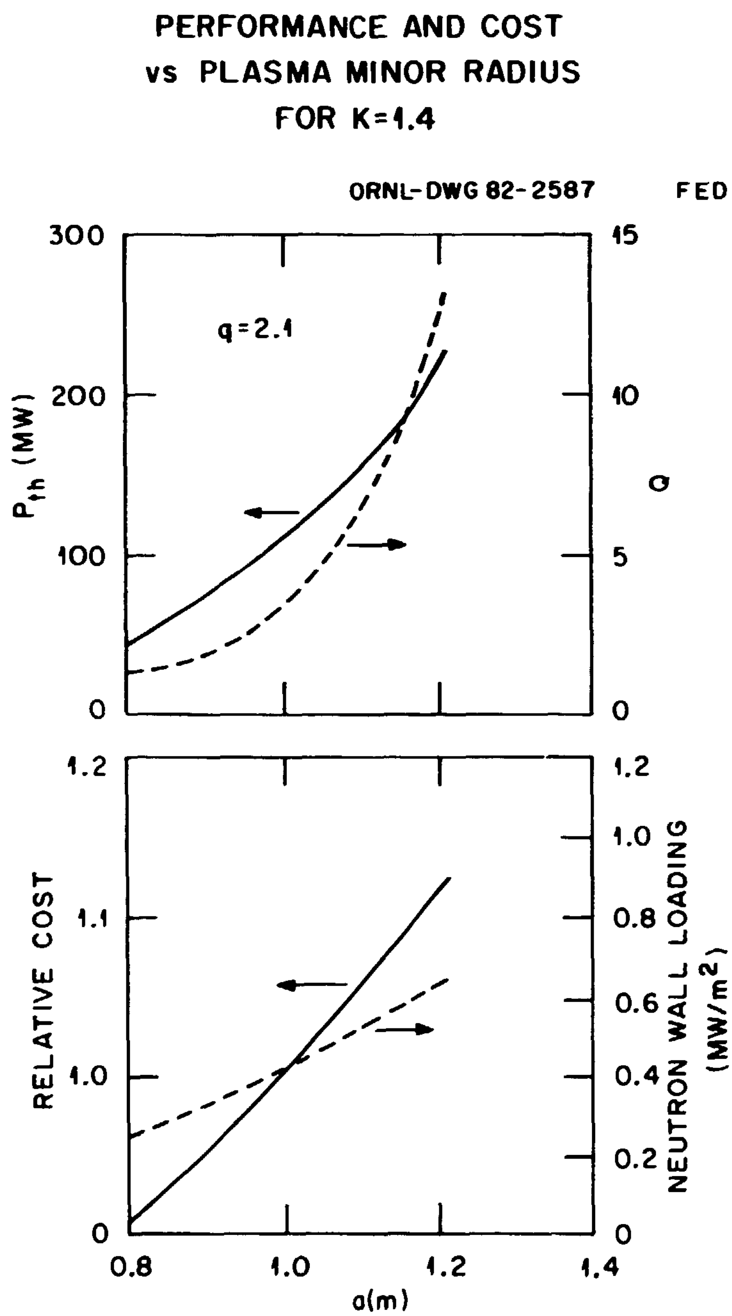
PERFORMANCE AND COST
vs PLASMA MINOR RADIUS
FOR K=1.4
ORNL-DWG 82-2587 FED
300
200
100
0
15
10
5
0
q=2.1
P th (MW)
Q
1.2
1.1
1.0
0
1.2
1.0
0.8
0.6
0.4
0.2
0
RELATIVE COST
NEUTRON WALL LOADING (MW/m2)
0.8
1.0
1.2
1.4
a(m)

Fig. 9

PERFORMANCE AND COST vs PLASMA MINOR RADIUS FOR K=1.6

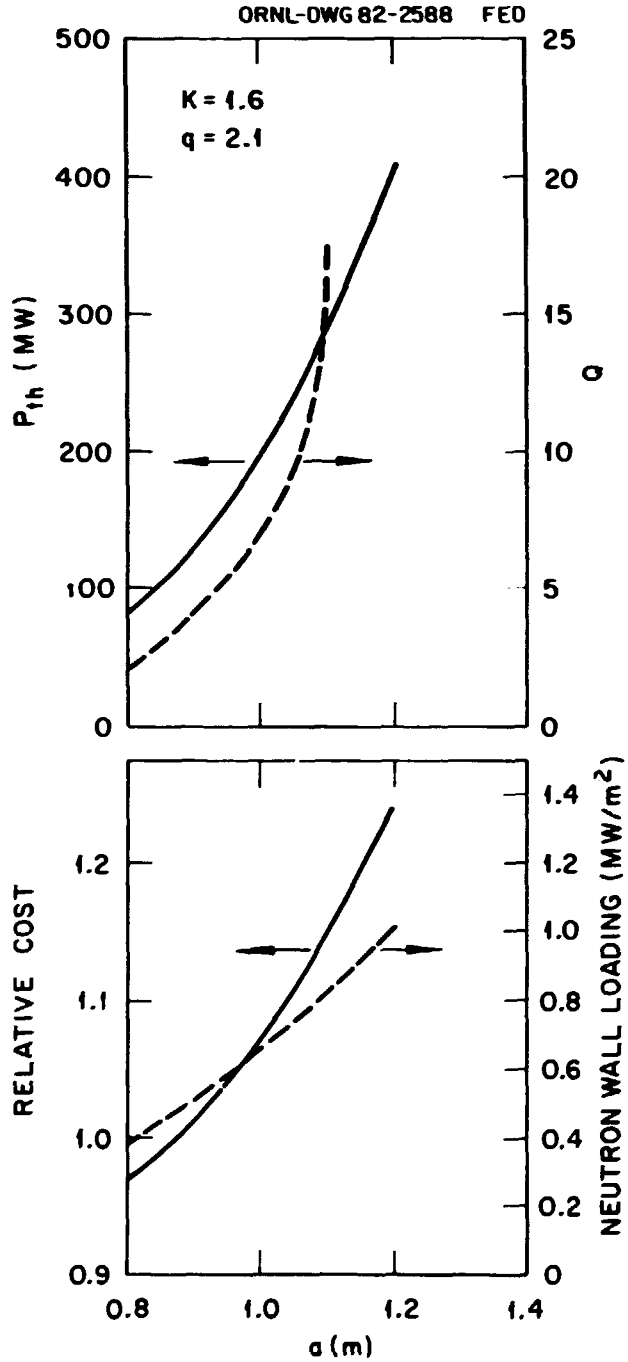

Fig. 10

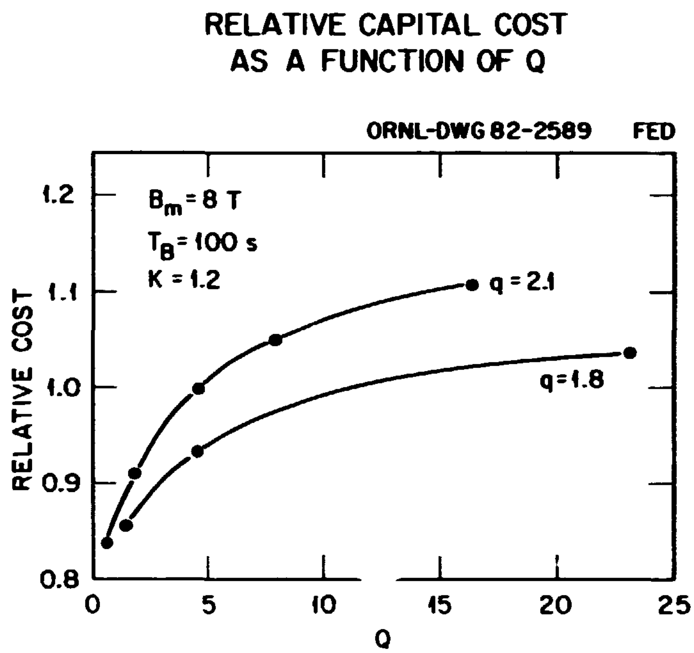
RELATIVE CAPITAL COST
AS A FUNCTION OF Q
ORNL-DWG 82-2589 FED
B_m = 8 T
T_B = 100 s
K = 1.2
q = 2.1
q = 1.8
RELATIVE COST
1.2
1.1
1.0
0.9
0.8
0
5
10
15
20
25
Q

Fig. 11

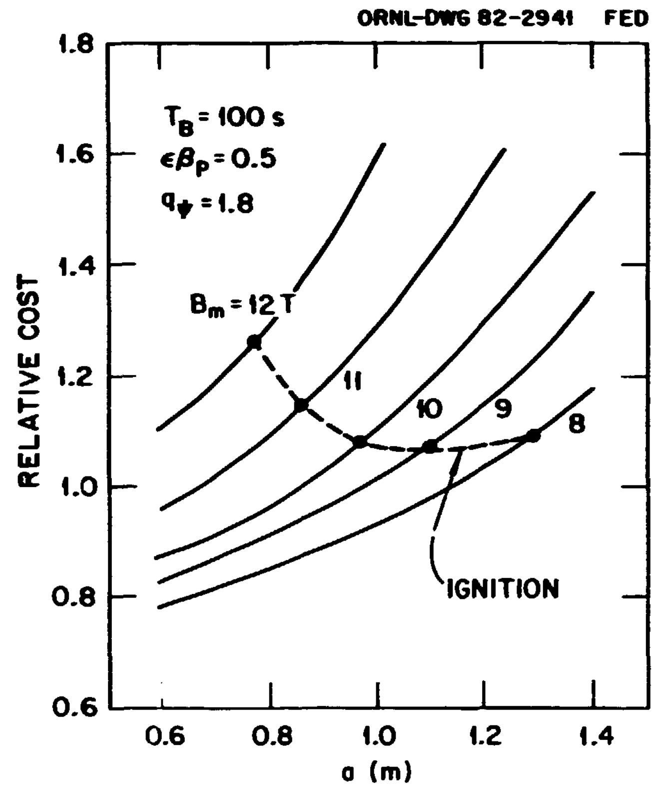
ORNL-DWG 82-2941 FED
1.8
1.6
1.4
1.2
1.0
0.8
0.6
RELATIVE COST
T_B = 100 s
$\epsilon\beta_p$ = 0.5
q_ψ = 1.8
B_m = 12 T
11
10
9
8
IGNITION
0.6
0.8
1.0
1.2
1.4
a (m)

Fig. 12

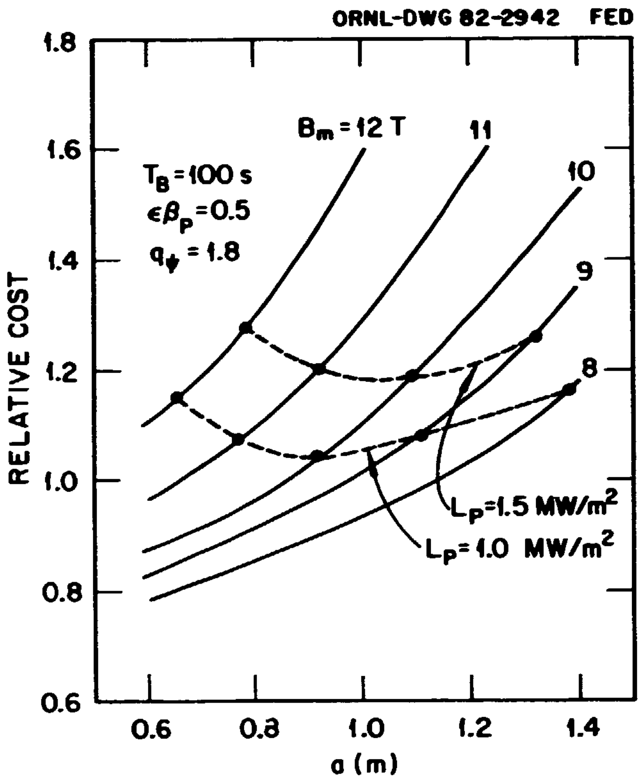
ORNL-DWG 82-2942 FED
RELATIVE COST
a (m)
B_m = 12 T
11
10
9
8
T_B = 100 s
$\epsilon\beta_p$ = 0.5
q_ψ = 1.8
L_p = 1.5 MW/m^2
L_p = 1.0 MW/m^2
1.8
1.6
1.4
1.2
1.0
0.8
0.6
0.6
0.8
1.0
1.2
1.4

Fig. 13

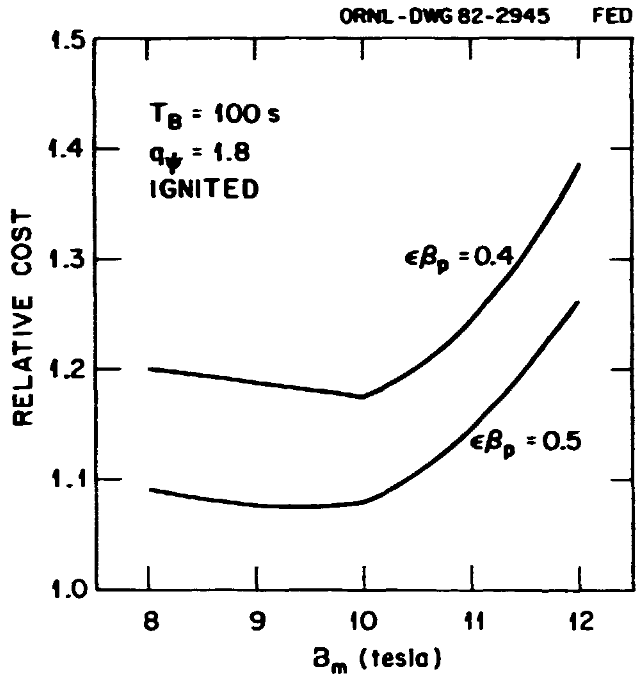
ORNL-DWG 82-2945 FED
1.5
1.4
1.3
1.2
1.1
1.0
RELATIVE COST
T_B = 100 s
q_ψ = 1.8
IGNITED
$\epsilon\beta_p$ = 0.4
$\epsilon\beta_p$ = 0.5
8
9
10
11
12
B_m (tesla)

Fig. 14

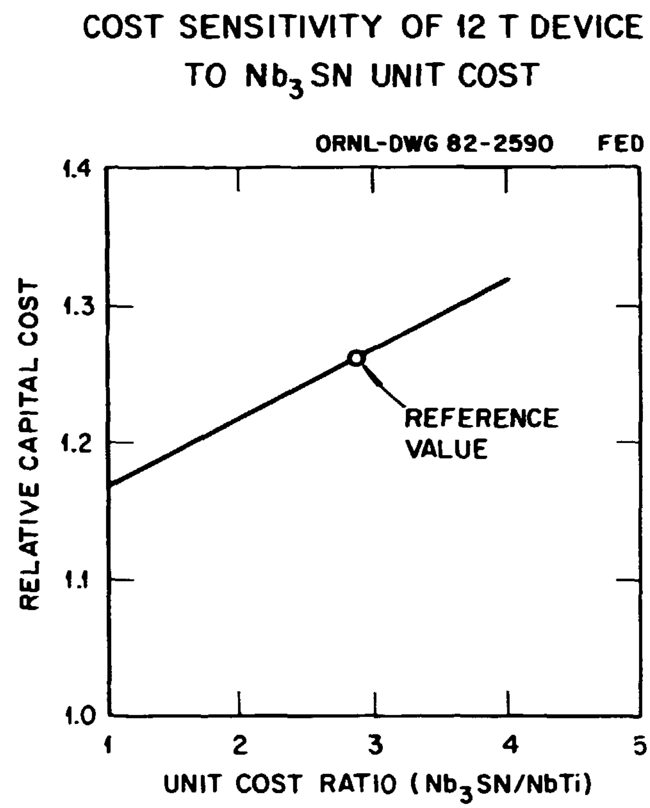
COST SENSITIVITY OF 12 T DEVICE
TO Nb3SN UNIT COST
ORNL-DWG 82-2590 FED
RELATIVE CAPITAL COST
1.4
1.3
1.2
1.1
1.0
REFERENCE
VALUE
1
2
3
4
5
UNIT COST RATIO (Nb3SN/NbTi)

Fig. 15

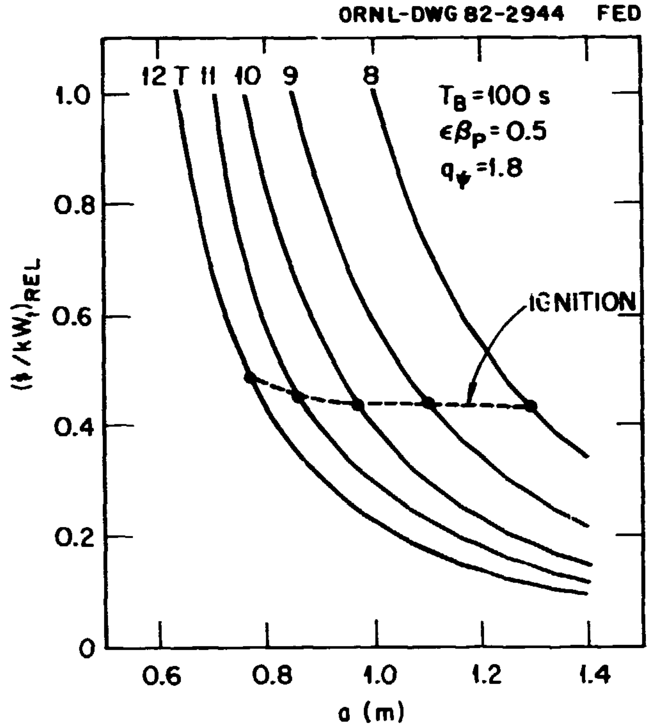
ORNL-DWG 82-2944 FED
12 T 11 10 9 8
$T_B = 100$ s
$\epsilon\beta_p = 0.5$
$q_\psi = 1.8$
IGNITION
$(\$/kW_t)_{REL}$
1.0
0.8
0.6
0.4
0.2
0
0.6
0.8
1.0
1.2
1.4
a (m)

Fig. 16

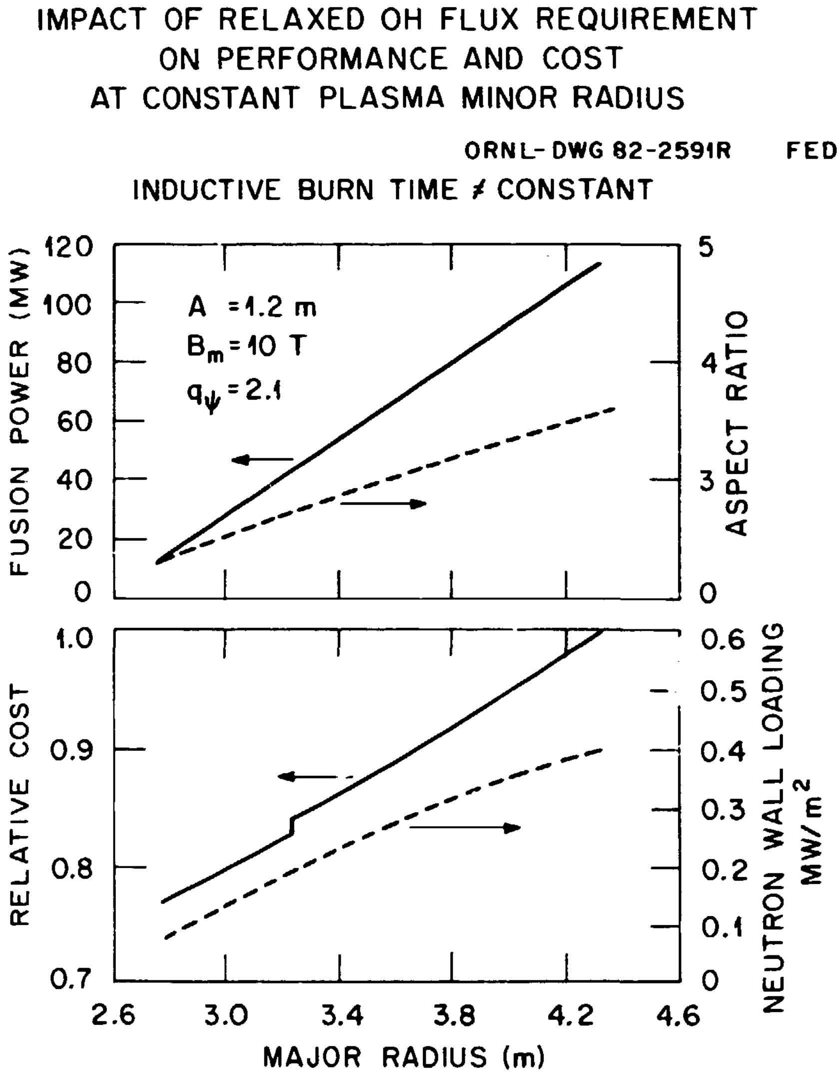
IMPACT OF RELAXED OH FLUX REQUIREMENT
ON PERFORMANCE AND COST
AT CONSTANT PLASMA MINOR RADIUS
ORNL-DWG 82-2591R FED
INDUCTIVE BURN TIME ≠ CONSTANT
A =1.2 m
B_m = 10 T
q_ψ = 2.1
FUSION POWER (MW)
ASPECT RATIO
RELATIVE COST
NEUTRON WALL LOADING MW/m^2
MAJOR RADIUS (m)
120
100
80
60
40
20
0
5
4
3
0
1.0
0.9
0.8
0.7
0.6
0.5
0.4
0.3
0.2
0.1
0
2.6
3.0
3.4
3.8
4.2
4.6

Fig. 17

IMPACT OF RELAXED OH FLUX REQUIREMENT ON PERFORMANCE AND COST AT CONSTANT NEUTRON WALL LOADING

ORNL-DWG 82-2592R FED

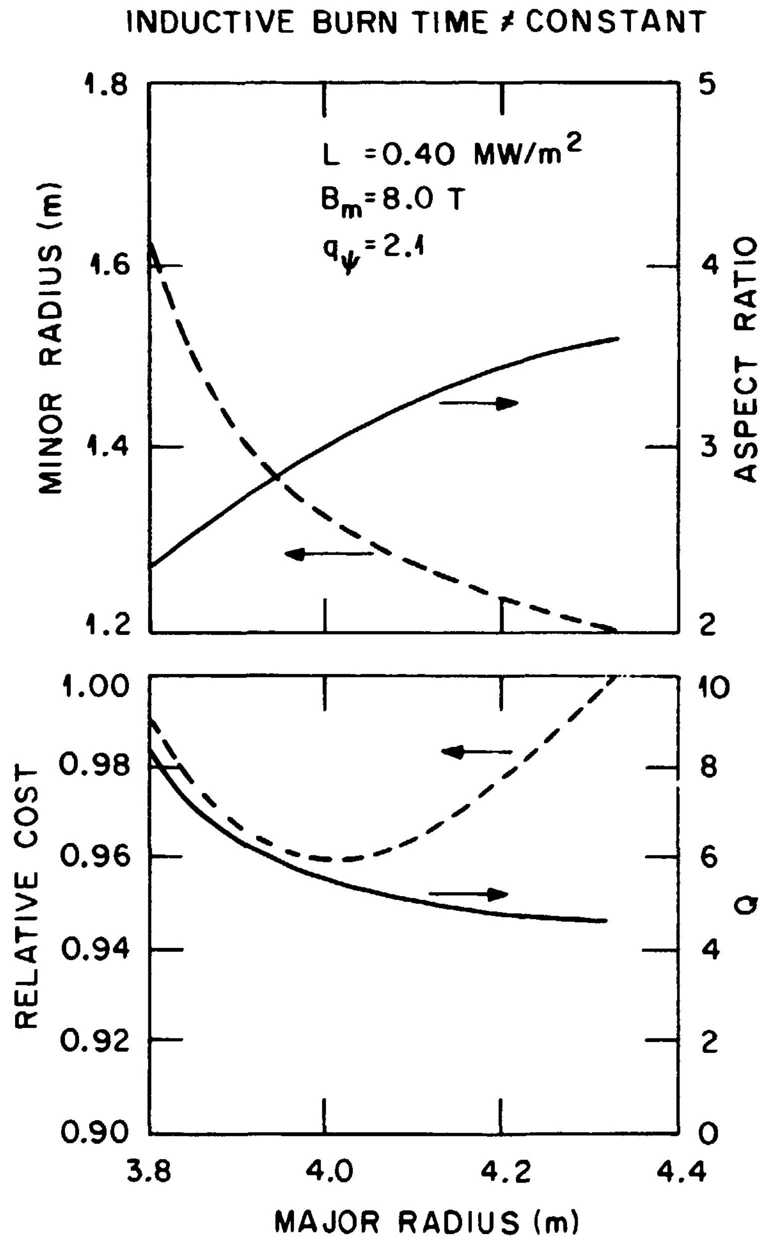

Fig. 18

ORNL-DWG 82-4126 FED

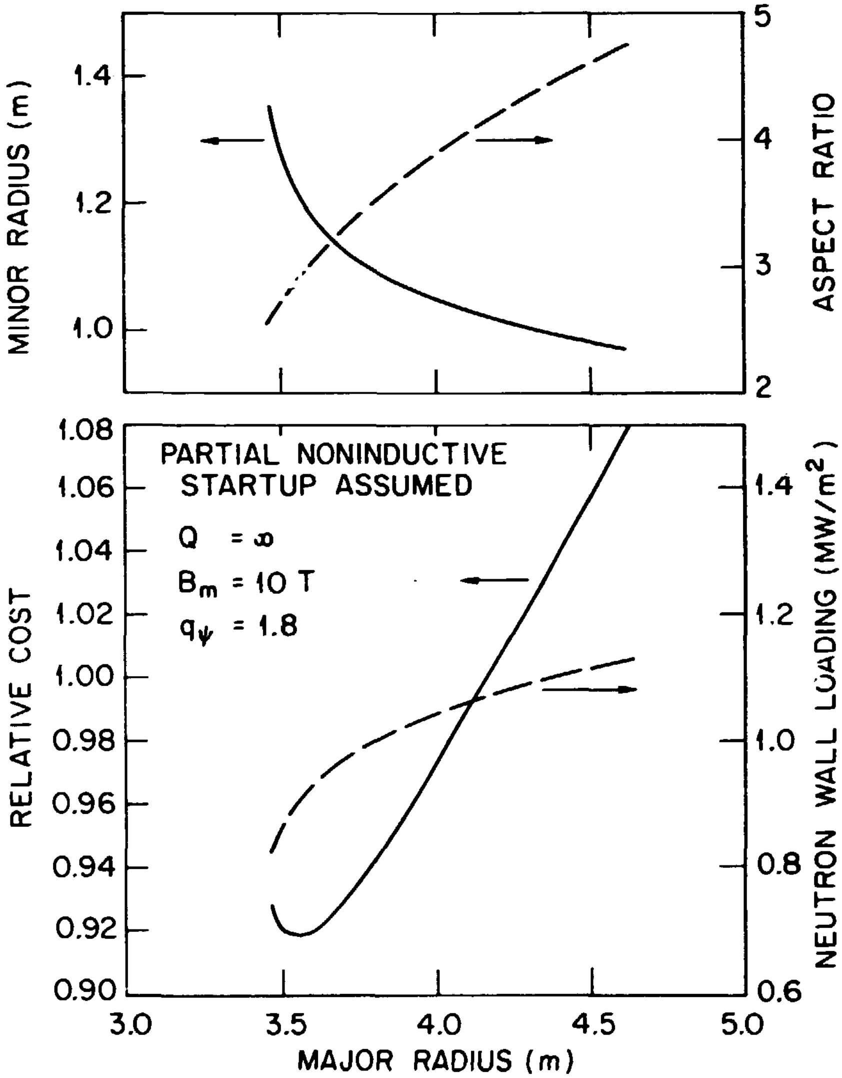

Fig. 19

ORNL/FEDC-83/3
Dist. Category UC-20 c,d

INTERNAL DISTRIBUTION

1. S. E. Attenberger
2. R. A. Dory
3. J. L. Dunlap
4. O. C. Eldridge
5. C. A. Flanagan
6. G. M. Fuller
7. P. King
8. J. A. O'Toole
9-13. Y-K. M. Peng
14-18. R. L. Reid
19. W. T. Reierson
20. J. A. Rome
21. T. E. Shannon
22. J. Sheffield
23. D. J. Sigmar
24. V. C. Srivastava
25. D. J. Strickler
26. N. A. Uckan
27. T. Uckan
28. F. W. Wiffen
29. F. Wu
30-31. Laboratory Records Department
32. Laboratory Records, ORNL-RC
33. Central Research Library
34. Fusion Energy Division Library
35. Fusion Energy Division Reports Office
36. ORNL Patent Office
37. Document Reference Section

EXTERNAL DISTRIBUTION

38. M. A. Abdou, Associate Director, FPP/207, Argonne National Laboratory, 9700 South Cass Avenue, Argonne, IL 60439
39. N. A. Amherd, Fusion Power Program, Advanced Systems Department, Electric Power Research Institute, P.O. Box 10412, Palo Alto, CA 94304
40. J. L. Anderson, CMB-3, Mail Stop 348, Los Alamos National Laboratory, P.O. Box 1663, Los Alamos, NM 87545
41. M. Anderson, Tennessee Valley Authority, 1300 Commerce Bank Building, Chattanooga, TN 37401
42. O. A. Anderson, Lawrence Berkeley Laboratory, University of California, Berkeley, CA 94720
43. D. J. Anthony, Advanced Power Program, Advanced Energy Programs Department, Building 2, Room 551, General Electric Company, Schenectady, NY 12345
44. C. C. Baker, FPP/208, Argonne National Laboratory, 9700 South Cass Avenue, Argonne, IL 60439
45. T. H. Batzer, L-536, Lawrence Livermore National Laboratory, P.O. Box 808, Livermore, CA 94550
46. J. E. Baublitz, Office of Fusion Energy, Department of Energy, Washington, DC 20545
47. W. Bauer, Physical Research Division, Sandia National Laboratories-Livermore, Livermore, CA 94550
48. J. F. Baur, GA Technologies, Inc., P.O. Box 81608, San Diego, CA 92138
49. D. S. Beard, Office of Fusion Energy, Office of Energy Research, Mail Stop G-256, U.S. Department of Energy, Washington, DC 20545

50. R. J. Beeley, ETEC, Rockwell International, P.O. Box 1449, Canoga Park, CA 91304
51. D. C. Berkey, Vice President & General Manager, Energy System and Technology Division, General Electric Company, P.O. Box 7600, Stamford, CT 06904
52. K. L. Black, Department E452, McDonnell Douglas Astronautics Company, P.O. Box 516, St. Louis, MO 63166
53. R. Botwin, C47-05, Grumman Aerospace Corporation, P.O. Box 31, Bethpage, NY 11714
54. W. B. Briggs, McDonnell Douglas Astronautics Company, P.O. Box 516, St. Louis, MO 63166
55. G. Bronner, Princeton Plasma Physics Laboratory, P.O. Box 451, Princeton, NJ 08544
56. J. N. Brooks, FPP/207, Argonne National Laboratory, 9700 South Cass Avenue, Argonne, IL 60439
57. S. C. Burnett, GA Technologies, Inc., P.O. Box 81608, San Diego, CA 92138
58. J. D. Callen, Department of Nuclear Engineering, University of Wisconsin, Madison, WI 53706
59. V. S. Chan, GA Technologies, Inc., P.O. Box 81608, San Diego, CA 92138
60. R. G. Clemmer, Fusion Power Program, Argonne National Laboratory, 9700 South Cass Avenue, Argonne, IL 60439
61. D. R. Cohn, MIT Plasma Fusion Center, 167 Albany Street, Cambridge, MA 02139
62. W. S. Cooper, Lawrence Berkeley Laboratory, University of California, Berkeley, CA 94720
63. J. W. Coursen, C36-05, Grumman Aerospace Corporation, P.O. Box 31, Bethpage, NY 11714
64. R. W. Conn, School of Chemical, Nuclear, and Thermal Engineering, Boelter Hall, University of California, Los Angeles, CA 90024
65. J. G. Crocker, EG&G Idaho, P.O. Box 1625, Idaho Falls, ID 83401
66. A. E. Dabiri, Energy Systems and Conservation Division, Science Applications, Inc., P.O. Box 2351, La Jolla, CA 92038
67. C. C. Damm, L-441, Lawrence Livermore National Laboratory, P.O. Box 808, Livermore, CA 94550
68. R. C. Davidson, Massachusetts Institute of Technology, 77 Massachusetts Avenue, Cambridge, MA 02139
69. N. A. Davies, Office of Fusion Energy, Office of Energy Research, Mail Station G-256, U.S. Department of Energy, Washington, DC 20545
70. J. W. Davis, E457, Building 81/1/B7, McDonnell Douglas Astronautics Company, P.O. Box 516, St. Louis, MO 63166
71. M. J. Davis, Sandia National Laboratories, P.O. Box 5800, Albuquerque, NM 87185
72. S. O. Dean, Director, Fusion Energy Development, Science Applications, Inc., 2 Professional Drive, Suite 249, Gaithersburg, MD 20760
73. J. F. Decker, Office of Fusion Energy, Department of Energy, Mail Stop G-256, Washington, DC 20545
74. D. DeFreece, E451, Building 81/1/B7, McDonnell Douglas Astronautics Company, P.O. Box 516, St. Louis, MO 63166

75. A. Deitz, Princeton Plasma Physics Laboratory, P.O. Box 451, Princeton, NJ 08544
76. D. A. Dingee, Program Manager, Fusion Technology, Pacific Northwest Laboratories, Battelle Boulevard, Richland, WA 99352
77. J. N. Doggett, L-441, Lawrence Livermore National Laboratory, P.O. Box 808, Livermore, CA 94550
78. H. Dreicer, Division Leader, CRT, Los Alamos National Laboratory, P.O. Box 1663, Los Alamos, NM 87545
79. D. Ehst, Argonne National Laboratory, 9700 South Cass Avenue, Argonne, IL 60439
80. G. A. Eliseev, I. V. Kurchatov Institute of Atomic Energy, P.O. Box 3402, 123182 Moscow, U.S.S.R.
81. W. R. Ellis, Office of Fusion Energy, Department of Energy, Mail Stop G-256, Washington, DC 20545
82. B. A. Engholm, GA Technologies, Inc., P.O. Box 81608, San Diego, CA 92138
83. H. P. Eubank, Princeton Plasma Physics Laboratory, P.O. Box 451, Princeton, NJ 08544
84. F. Farfaletti-Casali, Engineering Division, Joint Research Center, Ispra Establishment, 21020 Ispra (Varese), Italy
85. J. J. Ferrante, Manager, Building 36-241, Large Superconducting Program, General Electric Company, 1 River Road, Schenectady, NY 12345
86. J. File, Princeton Plasma Physics Laboratory, P.O. Box 451, Princeton, NJ 08544
87. P. A. Finn, Fusion Power Program, Argonne National Laboratory, 9700 South Cass Avenue, Argonne, IL 60439
88. H. K. Forsen, Bechtel Group, Inc., Research & Engineering, P.O. Box 3965, San Francisco, CA 94119
89. J. S. Foster, Jr., Building R4-2004, TRW Defense and Space Systems, 1 Space Park, Redondo Beach, CA 90278
90. T. K. Fowler, Associate Director for MFE, L-436, Lawrence Livermore National Laboratory, P.O. Box 808, Livermore, CA 94550
91. J. W. French, EBASCO Services, Inc., Forrestal Campus, CN-59, Princeton University, Princeton, NJ 08544
92. H. P. Furth, Director, Princeton Plasma Physics Laboratory, P.O. Box 451, Princeton, NJ 08544
93. J. G. Gavin, Jr., President, A01-11, Grumman Aerospace Corporation, P.O. Box 31, Bethpage, NY 11714
94. G. Gibson, Westinghouse Electric Corporation, Fusion Power Systems Department, P.O. Box 10864, Pittsburgh, PA 15236
95. J. R. Gilleland, Manager, Fusion Project, GA Technologies, Inc., P.O. Box 81608, San Diego, CA 92138
96. V. A. Glukhikh, Scientific-Research Institute of Electro-Physical Apparatus, 188631 Leningrad, U.S.S.R.
97. M. Y. Gohar, Argonne National Laboratory, 9700 South Cass Avenue, Argonne, IL 60439
98. W. D. Goins, Tennessee Valley Authority, 1300 Commerce Union Bank Building, Chattanooga, TN 37401
99. D. A. Goldberg, Lawrence Berkeley Laboratory, University of California, Berkeley, CA 94720

100. R. Goldston, Princeton Plasma Physics Laboratory, P.O. Box 451, Princeton, NJ 08544
101. M. B. Gottlieb, Princeton Plasma Physics Laboratory, P.O. Box 451, Princeton, NJ 08544
102. R. W. Gould, Department of Applied Physics, California Institute of Technology, Pasadena, CA 91109
103. M. W. Griffin, Department E236, McDonnell Douglas Astronautics Company, P.O. Box 516, St. Louis, MO 63166
104. C. R. Head, Office of Fusion Energy, Department of Energy, Mail Stop G-256, Washington, DC 20545
105. C. D. Henning, Lawrence Livermore National Laboratory, P.O. Box 808, Livermore, CA 94550
106. G. K. Hess, Office of Fusion Energy, Department of Energy, Mail Stop ER-701, Washington, DC 20545
107. T. Hiraoka, JT-60 Project Office I, Japan Atomic Energy Research Institute, Tokai Research Establishment, Tokai, Ibaraki, Japan
108. R. L. Hirsch, Manager, Synthetic Fuels Research, Exxon Research and Engineering Company, P.O. Box 4255, Baytown, TX 77520
109. J. J. Holmes, Westinghouse-Hanford Engineering Development Laboratory, P.O. Box 1970, Richland, WA 99352
110. W. G. Homeyer, GA Technologies, Inc., P.O. Box 81608, San Diego, CA 92138
111. J. C. Hosea, Princeton Plasma Physics Laboratory, P.O. Box 451, Princeton, NJ 08544
112. D. Hwang, Princeton Plasma Physics Laboratory, P.O. Box 451, Princeton, NJ 08544
113. G. J. Inukai, Department E231, McDonnell Douglas Astronautics Company, P.O. Box 516, St. Louis, MO 63166
114. D. L. Jassby, Princeton Plasma Physics Laboratory, P.O. Box 451, Princeton, NJ 08544
115. J. B. Joyce, Princeton Plasma Physics Laboratory, P.O. Box 451, Princeton, NJ 08544
116. R. A. Krakowski, CTR-12, Mail Stop 641, Los Alamos National Laboratory, P.O. Box 1663, Los Alamos, NM 87545
117. G. L. Kulcinski, University of Wisconsin, Department of Nuclear Engineering, Engineering Research Building, Room 439, 1500 Johnson Drive, Madison, WI 53706
118. D. L. Kummer, McDonnell Douglas Astronautics Company, P.O. Box 516, St. Louis, MO 63166
119. T. S. Latham, Mail Stop 44, United Technologies Research Center, Silver Lane, East Hartford, CT 06108
120. L. R. Ledman, Office of Fusion Energy, Department of Energy, Mail Stop G-256, Washington, DC 20545
121. L. M. Lidsky, MIT Plasma Fusion Center, 167 Albany Street, Cambridge, MA 02139
122. C. S. Liu, GA Technologies, Inc., P.O. Box 81608, San Diego, CA 92138
123. E. F. Lowell, General Manager, Energy Systems Programs Department, Building 2-455, General Electric Company, 1 River Road, Schenectady, NY 12345
124. D. J. McFarlin, Mail Stop 44, United Technologies Research Center, Silver Lane, East Hartford, CT 06108

125. R. McGrath, Fusion Power Program, Argonne National Laboratory, 9700 South Cass Avenue, Argonne, IL 60439
126. V. A. Maroni, CEN/205, Argonne National Laboratory, 9700 South Cass Avenue, Argonne, IL 60439
127. W. Marton, Office of Fusion Energy, Office of Energy Research, Mail Station G-256, U.S. Department of Energy, Washington, DC 20545
128. L. G. Masson, EG&G Idaho, Idaho National Engineering Laboratory, P.O. Box 1625, Idaho Falls, ID 83401
129. D. G. McAlees, Exxon Nuclear Company, Inc., 777 106th Avenue, NE, Bellevue, WA 98009
130. D. M. Meade, Princeton Plasma Physics Laboratory, P.O. Box 451, Princeton, NJ 08544
131. A. T. Mense, Building 107, Post B2, McDonnell Douglas Astronautics Company, P.O. Box 516, St. Louis, MO 63166
132. L. Michaels, Princeton Plasma Physics Laboratory, P.O. Box 451, Princeton, NJ 08544
133. D. Mikkelsen, Princeton Plasma Physics Laboratory, P.O. Box 451, Princeton, NJ 08544
134. R. L. Miller, GA Technologies, Inc., P.O. Box 81608, San Diego, CA 92138
135. R. G. Mills, Princeton Plasma Physics Laboratory, P.O. Box 451, Princeton, NJ 08544
136. J. T. D. Mitchell, Culham Laboratory, Abingdon, Oxon OX14 3DB, United Kingdom
137. R. W. Moir, Lawrence Livermore National Laboratory, P.O. Box 808, Livermore, CA 94550
138. D. B. Montgomery, MIT Plasma Fusion Center, 167 Albany Street, Cambridge, MA 02139
139. K. Moses, R-1/1078, TRW Defense and Space Systems, 1 Space Park, Recondo Beach, CA 90278
140. R. E. Muller, Aerojet Manufacturing Company, P.O. Box 4210, Fullerton, CA 92934
141. A. E. Munier, Grumman Aerospace Company, P.O. Box 31, Bethpage, NY 11714
142. M. R. Murphy, Office of Fusion Energy, Department of Energy, Washington, DC 20545
143. R. E. Nygren, FPP/207, Argonne National Laboratory, 9700 South Cass Avenue, Argonne, IL 60439
144. T. Ohkawa, GA Technologies, Inc., P.O. Box 81608, San Diego, CA 92138
145. M. Okabayashi, Princeton Plasma Physics Laboratory, P.O. Box 451, Princeton, NJ 08544
146. D. Overskei, GA Technologies, Inc., P.O. Box 81608, San Diego, CA 92138
147. R. R. Parker, Francis Bitter National Magnet Laboratory, 170 Albany Street, Cambridge, MA 02139
148. B. Pease, Culham Laboratory, Abingdon, Oxon OX14 3DB, United Kingdom
149. M. Pelovitz, Princeton Plasma Physics Laboratory, P.O. Box 451, Princeton, NJ 08544
150. F. W. Perkins, Princeton Plasma Physics Laboratory, P.O. Box 451, Princeton, NJ 08544

151. M. Petravic, Princeton Plasma Physics Laboratory, P.O. Box 451, Princeton, NJ 08544
152. M. Porkolab, Massachusetts Institute of Technology, 77 Massachusetts Avenue, Cambridge, MA 02139
153. D. E. Post, Princeton Plasma Physics Laboratory, P.O. Box 451, Princeton, NJ 08544
154. L. K. Price, Department of Energy, Oak Ridge Operations, P.O. Box E, Oak Ridge, TN 37830
155. R. E. Price, Office of Fusion Energy, Office of Energy Research, Mail Station G-256, Washington, DC 20545
156. D. H. Priester, Office of Fusion Energy, Department of Energy, Washington, DC 20545
157. F. A. Puhn, GA Technologies, Inc., P.O. Box 81608, San Diego, CA 92138
158. J. Purcell, GA Technologies, Inc., P.O. Box 81608, San Diego, CA 92138
159. R. V. Pyle, University of California, Lawrence Berkeley Laboratory, Berkeley, CA 94720
160. J. M. Rawls, GA Technologies, Inc., P.O. Box 81608, San Diego, CA 92138
161. P. J. Reardon, Princeton Plasma Physics Laboratory, P.O. Box 451, Princeton, NJ 08544
162. M. Roberts, Office of Fusion Energy, Department of Energy, Mail Stop G-256, Washington, DC 20545
163. J. D. Rogers, Los Alamos National Laboratory, P.O. Box 1663, Los Alamos, NM 87545
164. F. L. Robinson, Tennessee Valley Authority, 1300 Commerce Bank Building, Chattanooga, TN 37401
165. M. L. Rogers, Monsanto Research Corporation, Mound Laboratory Facility, P.O. Box 32, Miamisburg, OH 45342
166. M. N. Rosenbluth, RLM 11.218, Institute for Fusion Studies, University of Texas, Austin, TX 78712
167. L. Ruby, Lawrence Berkeley Laboratory, University of California, Berkeley, CA 94720
168. P. H. Rutherford, Princeton Plasma Physics Laboratory, P.O. Box 451, Princeton, NJ 08544
169. D. D. Ryutov, Institute of Nuclear Physics, Siberian Branch of the Academy of Sciences of the U.S.S.R., Sovetskaya St. 5, 630090 Novosibirsk, U.S.S.R.
170. M. M. Sabado, EBASCO Services, Inc., A Site, Building 1-A, Forrestal Campus, Princeton, NJ 08544
171. J. A. Schmidt, Princeton Plasma Physics Laboratory, P.O. Box 451, Princeton, NJ 08544
172. J. Schultz, MIT Plasma Fusion Center, 167 Albany Street, Cambridge, MA 02139
173. F. R. Scott, Electric Power Research Institute, P.O. Box 10412, Palo Alto, CA 94304
174. G. Sheffield, Princeton Plasma Physics Laboratory, P.O. Box 451, Princeton, NJ 08544
175. C. E. Singer, Princeton Plasma Physics Laboratory, P.O. Box 451, Princeton, NJ 08544

176. T. J. M. Sluyters, Accelerator Department, Brookhaven National Laboratory, Upton, NY 11973
177. D. Smith, Materials Science Division, Argonne National Laboratory, 9700 South Cass Avenue, Argonne, IL 60439
178. G. E. Smith, Grumman Aerospace Corporation, P.O. Box 31, Bethpage, NY 11714
179. R. I. Smith, Board Chairman, Public Service Electric and Gas Company, 80 Park Place, Newark, NJ 07101
180. L. Soroka, Lawrence Berkeley Laboratory, University of California, Berkeley, CA 94720
181. L. Southworth, GA Technologies, Inc., P.O. Box 81608, San Diego, CA 92138
182. I. Spighel, Lebedev Physical Institute, Leninsky Prospect 53, 117924 Moscow, U.S.S.R.
183. W. M. Stacey, Jr., Georgia Institute of Technology, School of Nuclear Engineering, Atlanta, GA 30332
184. E. Stern, Grumman Aerospace Corporation, CN-59, Forrestal Campus, Princeton, NJ 08544
185. L. D. Stewart, Princeton Plasma Physics Laboratory, P.O. Box 451, Princeton, NJ 08544
186. W. Stodiek, Princeton Plasma Physics Laboratory, P.O. Box 451, Princeton, NJ 08544
187. P. M. Stone, Office of Fusion Energy, Office of Energy Research, Mail Station G-256, Washington, DC 20545
188. I. N. Sviatoslavsky, Room 33, Engineering Research Building, 1500 Johnson Drive, University of Wisconsin, Madison, WI 53706
189. T. Tamano, GA Technologies, Inc., P.O. Box 81608, San Diego, CA 92138
190. R. E. Tatro, Manager, Energy Systems, M.Z. 16-1070, General Dynamics-Convair Division, P.O. Box 80847, San Diego, CA 92138
191. F. Tenney, Princeton Plasma Physics Laboratory, P.O. Box 451, Princeton, NJ 08544
192. F. Thomas, B-20-5, Grumman Aerospace Corporation, Bethpage, NY 11714
193. K. I. Thomassen, Lawrence Livermore National Laboratory, P.O. Box 808, Livermore, CA 94550
194. R. J. Thome, Francis Bitter National Magnet Laboratory, 170 Albany Street, Cambridge, MA 02139
195. S. L. Thomson, Bechtel Group, Inc., P.O. Box 3965, San Francisco, CA 94119
196. V. T. Tolok, Kharkov Physical-Technical Institute, Academical St. 1, 310108 Kharkov, U.S.S.R.
197. C. Trachsel, McDonnell Douglas Astronautics Company, P.O. Box 516, St. Louis, MO 63166
198. J. R. Treglio, General Dynamics-Convair Division, P.O. Box 80847, San Diego, CA 92138
199. A. W. Trivelpiece, Office of Energy Research, Department of Energy, Washington, DC 20545
200. L. R. Turner, Fusion Power Program, Argonne National Laboratory, 9700 South Cass Avenue, Argonne, IL 60439
201. M. A. Ulrickson, Princeton Plasma Physics Laboratory, P.O. Box 451, Princeton, NJ 08544

202. E. H. Valeo, Princeton Plasma Physics Laboratory, P.O. Box 451, Princeton, NJ 08544
203. T. C. Varljen, Westinghouse Electric Corporation, P.O. Box 10864, Pittsburgh, PA 15236
204. R. Varma, Physical Research Laboratory, Navrangpura, Ahmedabad, India
205. H. F. Vogel, Los Alamos National Laboratory, P.O. Box 1663, Los Alamos, NM 87545
206. A. Wait, Building 36-421, General Electric Company, 1 River Road, Schenectady, NY 12345
207. K. E. Wakefield, Princeton Plasma Physics Laboratory, P.O. Box 451, Princeton, NJ 08544
208. D. Weldon, Los Alamos National Laboratory, P.O. Box 1663, Los Alamos, NM 87545
209. J. C. Wesley, GA Technologies, Inc., P.O. Box 81608, San Diego, CA 92138
210. S. Whitley, Tennessee Valley Authority, 1300 Commerce Bank Building, Chattanooga, TN 37401
211. W. R. Wilkes, Monsanto Research Corporation, Mound Laboratory Facility, P.O. Box 32, Miamisburg, OH 45342
212. J. E. Wilkins, EG&G Idaho, Idaho National Engineering Laboratory, P.O. Box 1625, Idaho Falls, ID 83401
213. H. Willenberg, Mathematical Sciences Northwest, Inc., P.O. Box 1887, Bellevue, WA 98009
214. J. E. C. Williams, Francis Bitter National Magnet Laboratory, 170 Albany Street, Cambridge, MA 02139
215. P. Willis, Building 23, Room 298, General Electric Company, 1 River Road, Schenectady, NY 12345
216. T. F. Yang, MIT Plasma Fusion Center, 167 Albany Street, Cambridge, MA 02139
217. H. H. Yoshikawa, W/A-62, Hanford Engineering Development Laboratory, P.O. Box 1970, Richland, WA 99352
218. K. M. Young, Princeton Plasma Physics Laboratory, P.O. Box 451, Princeton, NJ 08544
219. N. E. Young, EBASCO Services, Inc., Princeton Plasma Physics Laboratory, P.O. Box 451, Princeton, NJ 08544
220. K. M. Zwilsky, National Materials Advisory Board, National Academy of Sciences, 2101 Constitution Avenue NW, Washington, DC 20418
221. Bibliothek, Max-Planck Institut fur Plasmaphysik, D-8046 Garching bei Munchen, Federal Republic of Germany
222. Bibliothek, Institut fur Plasmaphysik, KFA, Postfach 1913, D-5170 Julich, Federal Republic of Germany
223. Bibliotheque, Centre de Recherches en Physique des Plasmas, 21 Avenue des Bains, 1007 Lausanne, Switzerland
224. Bibliotheque, Service du Confinement des Plasmas, CEA, B.P. No. 6, 92 Fontenay-aux-Roses (Seine), France
225. Documentation S.I.G.N., Department de la Physique du Plasma et de la Fusion Controlee, Association EURATOM-CEA, Centre d'Etudes Nucleaires, B.P. 85, Centre du Tri, 38041 Grenoble, Cedex, France
226. Library, Centre de Recherches en Physique des Plasmas, 21 Avenue des Bains, 1007 Lausanne, Switzerland

227. Library, Culham Laboratory, UKAEA, Abingdon, Oxon, OX14 3DB, England
228. Library, FOM Institut voor Plasma-Fysica, Rijnhuizen, Jutphaas, Netherlands
229. Library, Institute of Physics, Academia Sinica, Beijing, Peoples Republic of China
230. Library, Institute for Plasma Physics, Nagoya University, Nagoya 464, Japan
231. Library, International Centre for Theoretical Physics, Trieste, Italy
232. Library, JET Joint Undertaking, Abingdon, Oxfordshire, OX14, DB, England
233. Library, Laboratoria Gas Ionizzati, Frascati, Italy
234. Plasma Research Laboratory, Australian National University, P.O. Box 4, Canberra, ACT 2000, Australia
235. Thermonuclear Library, Japan Atomic Energy Research Institute, Tokai, Naka, Ibaraki, Japan
236. Library, Plasma Physics Laboratory, Kyoto University, Gokasho Uji, Kyoto, Japan
237. Office of the Assistant Manager for Energy Research and Development, Department of Energy, Oak Ridge Operations, Oak Ridge, TN 37830

238-441. Given distribution as shown in TID-4500, Magnetic Fusion Energy (Distribution Category UC-20 c,d: Reactor Materials and Fusion Systems)